Regulation of Store-Operated Ca^{2+} Entry by IP_3 Receptors Independent of Their Ability to Release Ca^{2+}

Pragnya Chakraborty[1,2], Bipan Kumar Deb[1,3], Colin W. Taylor[4,*] and Gaiti Hasan[1,5,*]

[1]National Centre for Biological Sciences, Tata Institute of Fundamental Research, Bellary Road, Bangalore, 560065, India.

[2]SASTRA University, Thanjavur, Tamil Nadu, 613401, India.

[3]Present address: Department of Molecular and Cell Biology, University of California, Berkeley, CA, 94720, USA.

[4]Department of Pharmacology, University of Cambridge, Cambridge, CB2 1PD, UK.

[5]Lead Contact

[*]Correspondence: cwt1000@cam.ac.uk, gaiti@ncbs.res.in

ABSTRACT

Loss of endoplasmic reticular (ER) Ca^{2+} activates store-operated Ca^{2+} entry (SOCE) by causing the ER localized Ca^{2+} sensor STIM to unfurl domains that activate Orai channels in the plasma membrane at membrane contact sites (MCS). Here we demonstrate a novel mechanism by which the inositol 1,4,5 trisphosphate receptor (IP_3R), an ER-localized IP_3-gated Ca^{2+} channel, regulates neuronal SOCE. In human neurons, SOCE evoked by pharmacological depletion of ER-Ca^{2+} is attenuated by loss of IP_3Rs, and restored by expression of IP_3Rs even when they cannot release Ca^{2+}, but only if the IP_3Rs can bind IP_3. Imaging studies demonstrate that IP_3Rs enhance association of STIM1 with Orai1 in neuronal cells with empty stores; this requires an IP_3-binding site, but not a pore. Convergent regulation by IP_3Rs, may tune neuronal SOCE to respond selectively to receptors that generate IP_3.

Keywords: Ca^{2+} signaling, extended synaptotagmin, human neural progenitor cell, IP_3 receptor, membrane contact site, neuron, Orai, proximity ligation assay, STIM, store-operated Ca^{2+} entry

INTRODUCTION

The activities of all eukaryotic cells are regulated by increases in cytosolic free Ca^{2+} concentration ($[Ca^{2+}]_c$), which are almost invariably evoked by the opening of Ca^{2+}-permeable ion channels in biological membranes. The presence of these Ca^{2+} channels within the plasma membrane (PM) and the membranes of intracellular Ca^{2+} stores, most notably the endoplasmic reticulum (ER), allows cells to use both intracellular and extracellular sources of Ca^{2+} to evoke Ca^{2+} signals. In animal cells, the most widely expressed Ca^{2+} signaling sequence links extracellular stimuli, through their specific receptors and activation of phospholipase C, to formation of inositol 1,4,5-trisphosphate (IP_3), which then stimulates Ca^{2+} release from the ER through IP_3 receptors (IP_3R) (Foskett *et al.*, 2007; Prole and Taylor, 2019). IP_3Rs occupy a central role in Ca^{2+} signaling by releasing Ca^{2+} from the ER. IP_3Rs thereby elicit cytosolic Ca^{2+} signals, and by depleting the ER of Ca^{2+} they initiate a sequence that leads to activation of store-operated Ca^{2+} entry (SOCE) across the PM (Putney, 1986; Thillaiappan *et al.*, 2019). SOCE occurs when loss of Ca^{2+} from the ER causes Ca^{2+} to dissociate from the luminal Ca^{2+}-binding sites of an integral ER protein, stromal interaction molecule 1 (STIM1). STIM1 then unfolds its cytosolic domains to expose a region that binds directly to a Ca^{2+} channel within the PM, Orai, causing it to open and Ca^{2+} to flow into the cell across the PM (Parekh and Putney, 2005; Prakriya and Lewis, 2015; Lewis, 2020). The interactions between STIM1 and Orai occur across a narrow gap between the ER and PM, a membrane contact site (MCS), where STIM1 puncta trap Orai channels. While STIM1 and Orai are undoubtedly the core components of SOCE, many additional proteins modulate their interactions (Rosado,

Jenner and Sage, 2000; Palty *et al.*, 2012; Deb, Pathak and Hasan, 2016; Srivats *et al.*, 2016) and other proteins contribute by regulating the assembly of MCS (Chang *et al.*, 2013; Giordano *et al.*, 2013; Kang *et al.*, 2019).

It is accepted that IP_3-evoked Ca^{2+} release from the ER through IP_3Rs is the usual means by which extracellular stimuli evoke SOCE. Here, the role of the IP_3R is widely assumed to be restricted to its ability to mediate Ca^{2+} release from the ER and thereby activate STIM1. Evidence from *Drosophila*, where we suggested an additional role for IP_3Rs in regulating SOCE (Agrawal et al., 2010; Chakraborty et al., 2016), motivated the present study, wherein we examined the contribution of IP_3Rs to SOCE in mammalian neurons. We show that in addition to their ability to activate STIM1 by evoking ER Ca^{2+} release, IP_3Rs also facilitate interactions between active STIM1 and Orai1. This additional role for IP_3Rs, which is regulated by IP_3 but does not require a functional pore, reveals an unexpected link between IP_3, IP_3Rs and Ca^{2+} signaling that is not mediated by IP_3-evoked Ca^{2+} release. We speculate that dual regulation of SOCE by IP_3Rs may allow Ca^{2+} release evoked by IP_3 to be preferentially coupled to SOCE.

RESULTS

Loss of IP_3R1 Attenuates SOCE in Human Neural Stem Cells and Neurons

We investigated the effects of IP_3Rs on SOCE by measuring $[Ca^{2+}]_c$ in human neural stem cells and neurons prepared from embryonic stem cells. Human neural progenitor cells (hNPCs) were derived from H9 embryonic stem cells using small molecules that mimic cues provided during human brain development (Gopurappilly *et al.*, 2018). We

confirmed that hNPCs express canonical markers of neural stem cells (**Figure 1A**) and that IP_3R1 is the predominant IP_3R subtype (GEO accession no. GSE109111) (Gopurappilly *et al.*, 2018). An inducible lentiviral shRNA-miR construct targeting IP_3R1 reduced IP_3R1 expression by 93 ± 0.4% relative to a non-silencing (NS) construct (**Figures 1B and 1C**). Carbachol stimulates muscarinic acetylcholine receptors, which are expressed at low levels in hNPCs (Gopurappilly *et al.*, 2018). In Ca^{2+}-free medium, carbachol evoked an increase in $[Ca^{2+}]_c$ in about 10% of hNPCs, consistent with it stimulating Ca^{2+} release from the ER through IP_3Rs. Restoration of extracellular Ca^{2+} then evoked an increase in $[Ca^{2+}]_c$ in all cells that responded to carbachol. Both carbachol-evoked Ca^{2+} release and SOCE were abolished in hNPCs expressing IP_3R1-shRNA, confirming the effectiveness of the IP_3R1 knockdown (**Figure 1- figure supplement 1A-C**).

Thapsigargin, a selective and irreversible inhibitor of the ER Ca^{2+} pump (sarcoplasmic/endoplasmic reticulum Ca^{2+}-ATPase, SERCA), was used to deplete the ER of Ca^{2+} and thereby activate SOCE (**Figure 1D**) (Parekh and Putney, 2005). Restoration of extracellular Ca^{2+} to thapsigargin-treated hNPCs evoked a large increase in $[Ca^{2+}]_c$, reflecting the activity of SOCE (**Figure 1D**). The maximal amplitude and rate of SOCE were significantly reduced in cells lacking IP_3R1, but the resting $[Ca^{2+}]_c$ and thapsigargin-evoked Ca^{2+} release were unaffected (**Figures 1D-1F** and **Figure 1- figure supplement 1D and 1E**). STIM1 and Orai1 expression were also unaltered in hNPC lacking IP_3R1 (**Figure 1- figure supplement 1G**). After spontaneous differentiation of hNPC, cells expressed markers typical of mature neurons, and the cells responded to depolarization with an increase in $[Ca^{2+}]_c$ (**Figure**

1- figure supplement 1F and Figure 1- figure supplement 1H-J). Thapsigargin evoked SOCE in these differentiated neurons; and expression of IP_3R1-shRNA significantly reduced the SOCE response without affecting depolarization-evoked Ca^{2+} signals (**Figures 1H-1J** and **Figure 1- figure supplement 1H-1L**).

Loss of IP_3R1 Attenuates SOCE in Human Neuroblastoma Cells

IP_3Rs link physiological stimuli that evoke Ca^{2+} release from the ER to SOCE, but the contribution of IP_3Rs is thought to be limited to their ability to deplete the ER of Ca^{2+}. We have reported that in *Drosophila* neurons there is an additional requirement for IP_3Rs independent of ER Ca^{2+} release (Venkiteswaran and Hasan, 2009; Agrawal *et al.*, 2010; Chakraborty *et al.*, 2016). Our results with hNPCs and stem cell-derived neurons suggest a similar requirement for IP_3Rs in regulating SOCE in mammalian neurons. To explore the mechanisms underlying this additional role for IP_3Rs, we turned to a more tractable cell line, SH-SY5Y cells. These cells are derived from a human neuroblastoma; they exhibit many neuronal characteristics (Agholme *et al.*, 2010); they express M3 muscarinic acetylcholine receptors that evoke IP_3-mediated Ca^{2+} release and SOCE (Grudt, Usowicz and Henderson, 1996); and they express predominantly IP_3R1 (Wojcikiewicz, 1995; Tovey *et al.*, 2001), with detectable IP_3R3, but no IP_3R2 (**Figure 2A**). We used inducible expression of IP_3R1-shRNA to significantly reduce IP_3R1 expression (by 74 ± 1.2%), without affecting IP_3R3 (**Figures 2A and 2B**). As expected, carbachol-evoked Ca^{2+} signals in individual SH-SY5Y cells were heterogenous and the carbachol-evoked Ca^{2+} release was significantly reduced by knockdown of IP_3R1 (**Figures 2C and 2D** and **Figure 2 - figure supplement 1A**

and 1B). Thapsigargin evoked SOCE in SH-SY5Y cells (Grudt, Usowicz and Henderson, 1996), and it was significantly attenuated after knockdown of IP_3R1 without affecting resting $[Ca^{2+}]_c$, the Ca^{2+} release evoked by thapsigargin or expression of STIM1 and Orai1 (**Figures 2E-2G** and **Figure 2 - figure supplement 1C-1E**).

We also used CRISPR/Cas9n and Cas9 to disrupt one or both copies of the IP_3R1 gene, subsequently referred to as IKO (one copy knockout) and IKO null (both copies knocked out) in SH-SY5Y cells. IP_3R1 expression was absent in the IKO null (**Figure 2 - figure supplement 1F**) whereas expression of STIM1, STIM2 and Orai1 were unperturbed (**Figure 2 - figure supplement 1G**). Carbachol-evoked Ca^{2+} release and thapisgargin-evoked SOCE were significantly reduced (**Figure 2 - figure supplement 1H-1J**). Since the IKO null cells were fragile and grew slowly, we examined SOCE in SH-SY5Y cells with disruption of one copy of the IP_3R1 gene. In the IKO cells, IP_3R1 expression, carbachol-evoked Ca^{2+} signals and thapsigargin-evoked SOCE were all reduced. A minimal effect on thapsigargin-evoked store Ca^{2+} release was observed in IKO null and IKO cells (**Figure 2 - figure supplement 1J and 1Q**).

These observations, which replicate those from hNPCs and neurons (**Figure 1**), vindicate our use of SH-SY5Y cells to explore the mechanisms linking IP_3Rs to SOCE in human neurons.

Expression of IP_3R1 or IP_3R3 in SH-SY5Y cells expressing IP_3R1-shRNA restored both carbachol-evoked Ca^{2+} release and thapsigargin-evoked SOCE without affecting resting $[Ca^{2+}]_c$ or thapsigargin-evoked Ca^{2+} release (**Figures 2H-2J** and

Figure 2 - figure supplement 2A-2D). Over-expression of STIM1 in cells expressing NS-shRNA had no effect on SOCE (**Figure 2 - figure supplement 2E and 2F**), but it restored thapsigargin-evoked SOCE in cells expressing IP_3R1-shRNA, without affecting resting $[Ca^{2+}]_c$ or thapsigargin-evoked Ca^{2+} release (**Figures 2K-2M**). We conclude that IP_3Rs are required for optimal SOCE, but they are not essential because additional STIM1 can replace the need for IP_3Rs (**Figure 3A**).

It has been reported that SOCE is unaffected by loss of IP_3R in non-neuronal cells (Ma *et al.*, 2001; Chakraborty *et al.*, 2016). Consistent with these observations, the SOCE evoked in HEK cells by stores emptied fully by treatment with thapsigargin was unaffected by expression of IP_3R1 shRNA (**Figure 2 - figure supplement 3A-3C**) or by knockout of all three IP_3R subtypes using CRISPR/cas9 (HEK-TKO cells) (**Figure 2 - figure supplement 3D and 3E**). The association of STIM1 with Orai1 in wild type HEK cells and HEK TKO cells after thapsigargin-evoked store depletion also appeared identical as tested by a proximity ligation assay (PLA, described further in **Figure 5**) (**Figure 2 - figure supplement 3F**). Neuronal and non-neuronal cells may, therefore, differ in the contribution of IP_3R to SOCE. We return to this point later.

Binding of IP_3 to IP_3R Without a Functional Pore Stimulates SOCE

IP_3Rs are large tetrameric channels that open when they bind IP_3 and Ca^{2+}, but they also associate with many other proteins (Prole and Taylor, 2019), and many IP_3Rs within cells appear not to release Ca^{2+} (Thillaiappan *et al.*, 2019). A point mutation (D2550A, $IP_3R1^{D/A}$) within the IP_3R1 pore prevents it from conducting Ca^{2+} (Dellis *et al.*, 2008). As expected, expression of $IP_3R1^{D/A}$ in cells lacking IP_3R1 failed to rescue

carbachol-evoked Ca^{2+} release, but it unexpectedly restored thapsigargin-evoked SOCE (**Figures 3B-3D** and **Figure 3 - figure supplement 1A-E**). We confirmed that rescue of thapsigargin-evoked Ca^{2+} entry by this pore-dead IP_3R was mediated by a conventional SOCE pathway by demonstrating that it was substantially attenuated by siRNA-mediated knockdown of Orai1 (**Figures 3C and 3D** and **Figure 3 - figure supplement 1F-1H**).

Activation of IP_3Rs is initiated by IP_3 binding to the N-terminal IP_3-binding core of each IP_3R subunit (Prole and Taylor, 2019). Mutation of two conserved phosphate-coordinating residues in the α-domain of the binding core (R568Q and K569Q of IP_3R1, $IP_3R1^{RQ/KQ}$) almost abolishes IP_3 binding (Yoshikawa *et al.*, 1996; Iwai *et al.*, 2007), while mutation of a single residue (R568Q, IP_3R1^{RQ}) reduces the IP_3 affinity by ~10-fold (Dellis *et al.*, 2008). Expression of rat $IP_3R1^{RQ/KQ}$ rescued neither carbachol-evoked Ca^{2+} release nor thapsigargin-evoked SOCE in cells lacking IP_3R1 (**Figures 3E and 3F** and **Figure 3 - figure supplement 1C)**. However, expression of IP_3R1^{RQ} substantially rescued thapsigargin-evoked SOCE (**Figures 3E and 3F** and **Figure 3 - figure supplement 1I and 1J**). Expression of an N-terminal fragment of rat IP_3R (IP_3R1^{1-604}), to which IP_3 binds normally (Iwai *et al.*, 2007), failed to rescue thapsigargin-evoked SOCE (**Figure 3 - figure supplement 1K and 1L)**. These results establish that a functional IP_3-binding site within a full-length IP_3R is required for IP_3Rs to facilitate thapsigargin-evoked SOCE. Hence in cells with empty Ca^{2+} stores, IP_3 binding, but not pore-opening, is required for regulation of SOCE by IP_3Rs. In cells stimulated only with thapsigargin and expressing IP_3Rs with deficient IP_3 binding, basal levels of IP_3 are probably insufficient to meet this need.

We further examined the need for IP_3 by partially depleting the ER of Ca^{2+} using cyclopiazonic acid (CPA), a reversible inhibitor of SERCA, to allow submaximal activation of SOCE (**Figure 3 - figure supplement 1M and 1N**). Under these conditions, addition of carbachol in Ca^{2+}-free HBSS to cells expressing IP_3R1-shRNA caused a small increase in $[Ca^{2+}]_c$ (**Figures 4A-4C**). In the same cells expressing IP_3R1^{DA}, the carbachol-evoked Ca^{2+} release was indistinguishable from that observed in cells without IP_3R^{DA} (**Figures 4B and 4C**), indicating that the small response was entirely mediated by residual native IP_3R1 and/or IP_3R3. Hence, the experiment allows carbachol to stimulate IP_3 production in cells expressing IP_3R1^{DA} without causing additional Ca^{2+} release. The key result is that in cells expressing IP_3R1^{DA}, carbachol substantially increased SOCE (**Figures 4A-4C**). We conclude that IP_3, through IP_3Rs, regulates coupling of empty stores to SOCE. This is the first example of an IP_3R mediating a response to IP_3 that does not require the pore of the channel.

G-protein-coupled receptors are linked to IP_3 formation through the G-protein Gq, which stimulates phospholipase C β (PLC β). We used YM-254890 to inhibit Gq (Kostenis, Pfeil and Annala, 2020; Patt *et al.*, 2021). As expected, addition of YM-254890 to wild type (WT) or NS-shRNA transfected SH-SY5Y cells abolished the Ca^{2+} signals evoked by carbachol **(Figure 4 - figure supplement 1B)**, but it also reduced the maximal amplitude and rate of thapsigargin-evoked SOCE (**Figures 4D- 4E** and **Figure 3 - figure supplement 1O**). YM-254890 had no effect on the residual thapsigargin-evoked SOCE in SH-SY5Y cells expressing IP_3R1-shRNA **(Figure 4F** and **Figure 3 - figure supplement 1O**). The latter result is important because it

demonstrates that the inhibition of SOCE in cells with functional IP_3Rs is not an off-target effect causing a direct inhibition of SOCE.

In wild type or HEK-TKO cells, YM-254890 had no effect on thapsigargin-evoked SOCE, but it did inhibit SOCE in HEK cells lacking IP_3R1 (**Figures 4G-4I** and **Figure 4 - figure supplement 1C-1G**). These results suggest that in HEK cells, which normally express all three IP_3R subtypes (Mataragka & Taylor, 2018), neither loss of IP_3R1 nor inhibition of Gαq is sufficient on its own to inhibit thapsigargin-evoked SOCE, but when combined there is a synergistic loss of SOCE.

IP_3Rs Promote Interaction of STIM1 With Orai1 Within MCS

Our evidence that IP_3Rs intercept coupling between empty stores and SOCE (**Figure 3A**) prompted us to investigate the coupling of STIM1 with Orai1 across the narrow junctions between ER and PM (Carrasco and Meyer, 2011). An *in situ* proximity ligation assay (PLA) is well suited to analyzing this interaction because it provides a signal when two immunolabelled proteins are within ~40 nm of each other (Derangère *et al.*, 2016), a distance comparable to the dimensions of the junctions wherein STIM1 and Orai1 interact (Poteser *et al.*, 2016). We confirmed the specificity of the PLA and demonstrated that it reports increased association of STIM1 with Orai1 after treating SH-SY5Y cells with thapsigargin (**Figure 5A** and **Figure 5 - figure supplement 1A-1F**). In cells expressing IP_3R1-shRNA, thapsigargin had no effect on the STIM1-Orai1 interaction reported by PLA, but the interaction was rescued by expression of IP_3R1 or IP_3R1^{DA}. There was no rescue with $IP_3R1^{RQ/KQ}$ (**Figures 5B-5E**). WT SH-SY5Y cells that were depleted of basal IP_3 by treatment with the Gq inhibitor YM-254890,

showed significantly reduced STIM1-Orai1 interaction after thapsigargin-evoked depletion of Ca^{2+} stores (**Figure 4 - figure supplement 1A**). The results with PLA exactly mirror those from functional analyses (**Figures 1** to **4**), suggesting that IP_3 binding to IP_3R enhances SOCE by facilitating interaction of STIM1 with Orai1 (**Figure 3A**).

Extended synaptotagmins (E-Syts) are ER proteins that stabilize ER-PM junctions including STIM1-Orai1 MCS (Maléth *et al.*, 2014; Kang *et al.*, 2019; Woo *et al.*, 2020). Over-expression of E-Syt1 in SH-SY5Y cells expressing IP_3R1-shRNA rescued thapsigargin-evoked Ca^{2+} entry without affecting resting $[Ca^{2+}]_c$ or thapsigargin-evoked Ca^{2+} release (**Figures 6A-6C**). The rescued Ca^{2+} entry is likely to be mediated by conventional SOCE because it was substantially attenuated by knockdown of STIM1 (**Figures 6D-6F)**. Over-expression of E-Syt1 had no effect on SOCE in cells with unperturbed IP_3Rs (**Figures 6G-6I**). These results suggest that attenuated SOCE after loss of IP_3Rs can be restored by exaggerating ER-PM MCS.

DISCUSSION

After identification of STIM1 and Orai1 as core components of SOCE (Prakriya and Lewis, 2015; Thillaiappan *et al.*, 2019), the sole role of IP_3Rs within the SOCE pathway was assumed to be the release of ER Ca^{2+} that triggers STIM1 activation. The assumption is consistent with evidence that thapsigargin-evoked SOCE can occur in avian (Sugawara *et al.*, 1997; Ma *et al.*, 2002; Chakraborty *et al.*, 2016) and mammalian cells without IP_3Rs (Prakriya and Lewis, 2001). Although SOCE in

mammalian HEK cells was unaffected by loss of IP_3Rs in our study (**Figure 4G and 4I)**, it was modestly reduced in other studies of mammalian cells (Bartok *et al.*, 2019; Yue *et al.*, 2020). However, additional complexity is suggested by evidence that SOCE may be reduced in cells without IP_3Rs (Chakraborty *et al.*, 2016; Bartok *et al.*, 2019; Yue *et al.*, 2020), by observations implicating phospholipase C in SOCE regulation (Rosado, Jenner and Sage, 2000; Broad *et al.*, 2001), by evidence that SOCE responds differently to IP_3Rs activated by different synthetic ligands (Parekh, Riley and Potter, 2002) and by some, albeit conflicting reports (Woodard *et al.*, 2010; Santoso, Cebotaru and Guggino, 2011; Béliveau, Lessard and Guillemette, 2014; Sampieri *et al.*, 2018; Ahmad *et al.*, 2022), that IP_3Rs may interact with STIM and/or Orai (Woodard *et al.*, 2010; Santoso, Cebotaru and Guggino, 2011; Béliveau, Lessard and Guillemette, 2014; Sampieri *et al.*, 2018).

We identified two roles for IP_3Rs in controlling endogenous SOCE in human neurons. As widely reported, IP_3Rs activate STIM1 by releasing Ca^{2+} from the ER, but they also, and independent of their ability to release Ca^{2+}, enhance interactions between active STIM1 and Orai1 (**Figure 7**). The second role for IP_3Rs can be supplanted by over-expressing other components of the SOCE complex, notably STIM1 or ESyt1 (**Figures 2K-2M** and **Figures 6A and 6B**). It is intriguing that STIM1 (Carrasco and Meyer, 2011; Lewis, 2020), ESyt1 (Giordano *et al.*, 2013) and perhaps IP_3Rs (through the IP_3-binding core) interact with phosphatidylinositol 4,5-bisphosphate (PIP_2), which is dynamically associated with SOCE-MCS (Kang *et al.*, 2019). We suggest that the extent to which IP_3Rs tune SOCE in different cells is probably determined by the strength of Gq signaling and endogenous interactions

between STIM1 and Orai1. The latter is likely to depend on the relative expression of STIM1 and Orai1 (Woo *et al.*, 2020), the STIM isoforms expressed, expression of proteins that stabilize STIM1-Orai1 interactions (Darbellay *et al.*, 2011; Rana *et al.*, 2015; Rosado *et al.*, 2016; Knapp *et al.*, 2022), and the size and number of the MCS where STIM1 and Orai1 interact (Kang *et al.*, 2019). The multifarious contributors to SOCE suggest that cells may differ in whether they express "spare capacity". In neuronal cells, loss of IP_3 (**Figure 4D**) or of the dominant IP_3R isoform (IP_3R1-shRNA; **Figures 1 and 2**) is sufficient to unveil the contribution of IP_3R to SOCE, whereas HEK cells require loss of both IP_3 and IP_3R1 to unveil the contribution (**Figures 4H and 4I**). The persistence of SOCE in cells devoid of IP_3Rs (**Figure 2 - figure supplement 3D and 3E**) (Prakriya and Lewis, 2001; Ma *et al.*, 2002) probably arises from adaptive changes within the SOCE pathway. This does not detract from our conclusion that under physiological conditions, where receptors through IP_3 initiate SOCE, IP_3Rs actively regulate SOCE.

The IP_3Rs that initiate Ca^{2+} signals reside in ER immediately beneath the PM and alongside, but not within, the MCS where STIM1 accumulates after store depletion (Thillaiappan *et al.*, 2017). In migrating cells too, IP_3Rs and STIM1 remain separated as they redistribute to the leading edge (Okeke *et al.*, 2016). Furthermore, there is evidence that neither STIM1 nor STIM2 co-immmunoprecipitate with IP_3R1 (Ahmad *et al.*, 2022). We suggest, and consistent with evidence that SOCE in cells without IP_3Rs can be restored by over-expressing E-Syt1 (**Figures 6A-6C**), that IP_3Rs probably facilitate SOCE by stabilizing the MCS wherein STIM1 and Orai1 interact, rather than by directly regulating either protein. This proposal provides an analogy with similar

structural roles for IP_3Rs in maintaining MCS between ER and mitochondria (Bartok *et al.*, 2019) or lysosomes (Atakpa *et al.*, 2018) (**Figure 7C**). Since both contributions of IP_3Rs to SOCE require IP_3 binding (**Figures 3E and 3F**), each is ultimately controlled by receptors that stimulate IP_3 formation (**Figures 4B and 4C**). Convergent regulation by IP_3Rs at two steps in the SOCE pathway may ensure that receptor-regulated PLC activity provides the most effective stimulus for SOCE; more effective, for example, than ryanodine receptors, which are also expressed in neurons (**Figure 7B**). By opening IP_3Rs parked alongside SOCE MCS (Thillaiappan *et al.*, 2017; Ahmad *et al.*, 2022), IP_3 selectively releases Ca^{2+} from ER that is optimally placed to stimulate SOCE, and by facilitating Orai1-STIM1 interactions IP_3 reinforces this local activation of SOCE (**Figure 7A and 7B**).

We conclude that IP_3-regulated IP_3Rs regulate SOCE by mediating Ca^{2+} release from the ER, thereby activating STIM1 and/or STIM2 (Ahmad *et al.*, 2022) and, independent of their ability to release Ca^{2+}, IP_3Rs facilitate the interactions between STIM and Orai that activate SOCE. Dual regulation of SOCE by IP_3 and IP_3Rs allows robust control by cell-surface receptors and may reinforce local stimulation of Ca^{2+} entry.

ACKNOWLEDGEMENTS

This research was supported by grants to G.H. from the Dept. of Biotechnology, Govt. of India (BT/PR6371/COE/34/19/2013) and NCBS-TIFR core support, and to C.W.T. from the Wellcome Trust (101844) and Biotechnology and Biological Sciences

Research Council (BB/T012986/1). P.C is supported by a DST-INSPIRE fellowship (DST/INSPIRE Fellowship/2017/IF170360) and she received an Infosys-NCBS travel award to visit C.W.T.'s lab at Cambridge. We are grateful to Renjitha Gopurappilly (NCBS, TIFR) for the derivation of human neural precursor cells. We acknowledge use of the Central Imaging and Flow Cytometry Facility (CIFF), Stem Cell Culture Facility and Biosafety level-2 laboratory facility at NCBS, TIFR.

DISCLOSURE AND COMPETING INTEREST STATEMENT

The authors declare no competing interests.

REFERENCES

Agholme, L., Lindström, T., Kågedal, K., Marcusson, J. and Hallbeck, M. 2010. An in vitro model for neuroscience: differentiation of SH-SY5Y cells into cells with morphological and biochemical characteristics of mature neurons. *J. Alzheimer's Dis.* 20:1069–1082.

Agrawal, N., Venkiteswaran, G., Sadaf, S., Padmanabhan, N., Banerjee, S. and Hasan, G. 2010. Inositol 1, 4, 5-trisphosphate receptor and dSTIM function in *Drosophila* insulin-producing neurons regulates systemic intracellular calcium homeostasis and flight. *J. Neurosci*. 30:1301-1313.

Ahmad, M. et al. 2022. Functional communication between IP_3R and STIM2 at subthreshold stimuli is a critical checkpoint for initiation of SOCE. *Proc. Natl. Acad. Sci.* 119: e2114928118.

Atakpa, P., Thillaiappan, N.B., Mataragka, S., Prole, D.L. and Taylor, C.W. 2018. IP_3

receptors preferentially associate with ER-lysosome contact sites and selectively deliver Ca^{2+} to lysosomes. *Cell Rep.* 25:3180-3193.

Auyeung, V.C., Ulitsky, I., McGeary, S.E. and Bartel, D.P. 2013. Beyond secondary structure: primary-sequence determinants license pri-miRNA hairpins for processing. *Cell.* 152:844-858.

Bartok, A., Weaver, D., Golenár, T., Nichtova, Z., Katona, M., Bánsághi, S., Alzayady, K.J., Thomas, V.K., Ando, H., Mikoshiba, K. and Joseph, S.K. 2019. IP_3 receptor isoforms differently regulate ER-mitochondrial contacts and local calcium transfer. *Nat. Commun*. 10:1-14.

Béliveau, É., Lessard, V. and Guillemette, G. 2014. STIM1 positively regulates the Ca^{2+} release activity of the inositol 1,4,5-trisphosphate receptor in bovine aortic endothelial cells. *PLoS One.* 9: e114718.

Broad, L.M., Braun, F.J., Lievremont, J.P., Bird, G.S.J., Kurosaki, T. and Putney Jr, J.W. 2001. Role of the phospholipase C-inositol 1, 4, 5-trisphosphate pathway in calcium release-activated calcium current and capacitative calcium entry. *J. Biol. Chem.* 276:15945–15952.

Carrasco, S. and Meyer, T. 2011. STIM proteins and the endoplasmic reticulum-plasma membrane junctions. *Annu. Rev. Biochem.* 80:973–1000.

Chakraborty, S., Deb, B.K., Chorna, T., Konieczny, V., Taylor, C.W. and Hasan, G. 2016. Mutant IP_3 receptors attenuate store-operated Ca^{2+} entry by destabilizing STIM–Orai interactions in *Drosophila* neurons. *J. Cell Sci.* 129:3903–3910.

Chang, C.L., Hsieh, T.S., Yang, T.T., Rothberg, K.G., Azizoglu, D.B., Volk, E., Liao, J.C. and Liou, J. 2013. Feedback regulation of receptor-induced Ca^{2+} signaling

mediated by E-Syt1 and Nir2 at endoplasmic reticulum-plasma membrane junctions. *Cell Rep*. 5:813–825.

Darbellay, B., Arnaudeau, S., Bader, C.R., Konig, S. and Bernheim, L. 2011. STIM1L is a new actin-binding splice variant involved in fast repetitive Ca^{2+} release. *J. Cell Biol.* 194:335-346.

Deb, B. K., Pathak, T. and Hasan, G. 2016. Store-independent modulation of Ca^{2+} entry through Orai by Septin 7. *Nat. Commun.* 7:1-15.

Dellis, O., Rossi, A.M., Dedos, S.G. and Taylor, C.W. 2008. Counting functional inositol 1, 4, 5-trisphosphate receptors into the plasma membrane. *J Biol. Chem.* 283:751-755.

Derangère, V., Bruchard, M., Végran, F. and Ghiringhelli, F. 2016. Proximity Ligation Assay (PLA) protocol using Duolink® for T cells. *Bio-protocol.* 6:e1811.

Forostyak, O., Romanyuk, N., Verkhratsky, A., Sykova, E. and Dayanithi, G. 2013. Plasticity of calcium signaling cascades in human embryonic stem cell-derived neural precursors. *Stem Cells Dev.* 22:1506-1521.

Foskett, J.K., White, C., Cheung, K.H. and Mak, D.O.D. 2007. Inositol trisphosphate receptor Ca^{2+} release channels. *Physiol. Rev.* 87:593–658.

Giordano, F., Saheki, Y., Idevall-Hagren, O., Colombo, S.F., Pirruccello, M., Milosevic, I., Gracheva, E.O., Bagriantsev, S.N., Borgese, N. and De Camilli, P. 2013. PI(4, 5) P_2-dependent and Ca^{2+}-regulated ER-PM interactions mediated by the extended synaptotagmins. *Cell*. 153:1494-1509.

Gopurappilly, R., Deb, B.K., Chakraborty, P. and Hasan, G. 2018. Stable STIM1 knockdown in self-renewing human neural precursors promotes premature

neural differentiation. *Front. Mol. Neurosci.* 11:178.

Grudt, T. J., Usowicz, M. M. and Henderson, G. 1996. Ca^{2+} entry following store depletion in SH-SY5Y neuroblastoma cells. *Mol. Brain Res.* 36:93–100.

Grynkiewicz, G., Poenie, M. and Tsien, R. Y. 1985. A new generation of Ca^{2+} indicators with greatly improved fluorescence properties. *J. Biol. Chem.* 260:3440–3450.

Iwai, M., Michikawa, T., Bosanac, I., Ikura, M. and Mikoshiba, K. 2007. Molecular basis of the isoform-specific ligand-binding affinity of inositol 1, 4, 5-trisphosphate receptors. *J. Biol. Chem.* 282:12755–12764.

Kang, F., Zhou, M., Huang, X., Fan, J., Wei, L., Boulanger, J., Liu, Z., Salamero, J., Liu, Y. and Chen, L. 2019. E-syt1 Re-arranges STIM1 clusters to stabilize ring-shaped ER-PM contact sites and accelerate Ca^{2+} store replenishment. *Sci Rep.* 9:1-11.

Knapp, M.L., Alansary, D., Poth, V., Förderer, K., Sommer, F., Zimmer, D., Schwarz, Y., Künzel, N., Kless, A., Machaca, K. and Helms, V., 2022. A longer isoform of Stim1 is a negative SOCE regulator but increases cAMP-modulated NFAT signaling. *EMBO reports*, *23:* e53135.

Knott, S.R., Maceli, A.R., Erard, N., Chang, K., Marran, K., Zhou, X., Gordon, A., El Demerdash, O., Wagenblast, E., Kim, S. and Fellmann, C. 2014. A computational algorithm to predict shRNA potency. *Mol. Cell.* 56:796-807.

Lewis, R. S. 2020. Store-operated calcium channels: From function to structure and back again. *Cold Spring Harb. Perspect. Biol.* 12: a035055.

Ma, H. T., Venkatachalam, K., Li, H. S., Montell, C., Kurosaki, T., Patterson, R. L., &

Gill, D. L. 2001. Assessment of the role of the inositol 1,4,5-trisphosphate receptor in the activation of transient receptor potential channels and store-operated Ca^{2+} entry channels. *J Biol Chem*, 276: 18888–18896.

Ma, H. T., Venkatachalam, K., Parys, J. B., & Gill, D. L. 2002. Modification of store-operated channel coupling and inositol trisphosphate receptor function by 2-aminoethoxydiphenyl borate in DT40 lymphocytes. *J Biol Chem*, 277: 6915–6922.

Maléth, J., Choi, S., Muallem, S. and Ahuja, M. 2014. Translocation between PI(4, 5)P_2-poor and PI(4, 5)P_2-rich microdomains during store depletion determines STIM1 conformation and Orai1 gating. *Nat Commun.* 5:1–10.

Mataragka, S. and Taylor, C. W. 2018. All three IP_3 receptor subtypes generate Ca^{2+} puffs, the universal building blocks of IP_3-evoked Ca^{2+} signals. *J Cell Sci.* 131: jcs220848.

Miotke, L., Lau, B. T., Rumma, R. T., & Ji, H. P. 2014. High sensitivity detection and quantitation of DNA copy number and single nucleotide variants with single color droplet digital PCR. *Anal. Chem.*, *86:* 2618-2624.

Nunes-Hasler, P., Maschalidi, S., Lippens, C., Castelbou, C., Bouvet, S., Guido, D., Bermont, F., Bassoy, E.Y., Page, N., Merkler, D. and Hugues, S. 2017. STIM1 promotes migration, phagosomal maturation and antigen cross-presentation in dendritic cells. *Nat Commun*. 8:1-15.

Okeke, E., Parker, T., Dingsdale, H., Concannon, M., Awais, M., Voronina, S., Molgó, J., Begg, M., Metcalf, D., Knight, A.E. and Sutton, R. 2016. Epithelial–mesenchymal transition, IP_3 receptors and ER–PM junctions: Translocation of

Ca^{2+} signalling complexes and regulation of migration. *Biochem. J*. 473:757–767.

Palty, R., Raveh, A., Kaminsky, I., Meller, R. and Reuveny, E. 2012. SARAF inactivates the store operated calcium entry machinery to prevent excess calcium refilling. *Cell*. 149:425-438.

Parekh, A. B. and Putney, J. W. 2005. Store-operated calcium channels. *Physiol. Rev.* 85:757–810.

Parekh, A. B., Riley, A. M. and Potter, B. V. L. 2002. Adenophostin A and ribophostin, but not inositol 1,4,5-trisphosphate or manno-adenophostin, activate the Ca^{2+} release-activated Ca^{2+} current, ICRAC, in weak intracellular Ca^{2+} buffer. *Biochem. J*. 361:133–141.

Patt, J., Alenfelder, J., Pfeil, E.M., Voss, J.H., Merten, N., Eryilmaz, F., Heycke, N., Rick, U., Inoue, A., Kehraus, S. and Deupi, X. 2021. An experimental strategy to probe Gq contribution to signal transduction in living cells. *J. Biol. Chem.* 296:100472.

Poteser, M., Leitinger, G., Pritz, E., Platzer, D., Frischauf, I., Romanin, C. and Groschner, K. 2016. Live-cell imaging of ER-PM contact architecture by a novel TIRFM approach reveals extension of junctions in response to store-operated Ca^{2+}-entry. *Sci. Rep*. 6:1-13.

Prakriya, M. and Lewis, R. S. 2001. Potentiation and inhibition of Ca^{2+} release-activated Ca^{2+} channels by 2-aminoethyldiphenyl borate (2-APB) occurs independently of IP_3 receptors. *J Physiol*. 536:3–19.

Prakriya, M. and Lewis, R. S. 2015. Store-operated calcium channels pharmacology. *Physiol. Rev.* 307:1383–1436.

Prole, D. L. and Taylor, C. W. 2019. Structure and function of IP_3 receptors. *Cold Spring Harb. Perspect. Biol.* 11: a035063.

Putney, J. W. 1986. A model for receptor-regulated calcium entry. *Cell Calcium*. 7:1–12.

Ran, F. A., Hsu, P. D., Wright, J., Agarwala, V., Scott, D. A., & Zhang, F. 2013. Genome engineering using the CRISPR-Cas9 system. *Nat. Protoc*. 8: 2281-2308.

Rana, A., Yen, M., Sadaghiani, A.M., Malmersjö, S., Park, C.Y., Dolmetsch, R.E. and Lewis, R.S. 2015. Alternative splicing converts STIM2 from an activator to an inhibitor of store-operated calcium channels. *J Cell Biol.* 209: 653-670.

Reinhardt, P., Glatza, M., Hemmer, K., Tsytsyura, Y., Thiel, C.S., Höing, S., Moritz, S., Parga, J.A., Wagner, L., Bruder, J.M. and Wu, G. 2013. Derivation and expansion using only small molecules of human neural progenitors for neurodegenerative disease modeling. *PLoS One.* 8: e59252.

Rosado, J.A., Diez, R., Smani, T. and Jardín, I. 2016. STIM and Orai1 variants in store-operated calcium entry. *Front. Pharmacol.* 6:325.

Rosado, J. A., Jenner, S. and Sage, S. O. 2000. A role for the actin cytoskeleton in the initiation and maintenance of store-mediated calcium entry in human platelets. Evidence for conformational coupling. *J Biol. Chem*. 275: 7527–7533.

Saleem, H., Tovey, S.C., Rahman, T., Riley, A.M., Potter, B.V. and Taylor, C.W. 2013. Stimulation of inositol 1, 4, 5-trisphosphate (IP_3) receptor subtypes by analogues of IP_3. *PLoS One.* 8:e54877.

Sampieri, A., Santoyo, K., Asanov, A. and Vaca, L. 2018. Association of the IP_3R to

STIM1 provides a reduced intraluminal calcium microenvironment, resulting in enhanced store-operated calcium entry. *Sci Rep*. 8:1–13.

Santoso, N. G., Cebotaru, L. and Guggino, W. B. 2011. Polycystin-1, 2, and STIM1 interact with IP_3R to modulate ER Ca^{2+} release through the PI3K/Akt pathway. *Cell Physiol Biochem*. 27:715–726.

Srivats, S., Balasuriya, D., Pasche, M., Vistal, G., Edwardson, J.M., Taylor, C.W. and Murrell-Lagnado, R.D. 2016. Sigma-1 receptors inhibit store-operated Ca^{2+} entry by attenuating coupling of STIM1 to Orai1. *J. Cell Biol.* 213: 65–79.

Sugawara, H., Kurosaki, M., Takata, M. and Kurosaki, T. 1997. Genetic evidence for involvement of type 1, type 2 and type 3 inositol 1, 4, 5-trisphosphate receptors in signal transduction through the B-cell antigen receptor. *EMBO J*. 16:3078–3088.

Thillaiappan, N.B., Chavda, A.P., Tovey, S.C., Prole, D.L. and Taylor, C.W. 2017. Ca^{2+} signals initiate at immobile IP_3 receptors adjacent to ER-plasma membrane junctions. *Nat. Commun.* 8:1-16.

Thillaiappan, N.B., Chakraborty, P., Hasan, G. and Taylor, C.W. 2019. IP_3 receptors and Ca^{2+} entry. *Biochim Biophys Acta Mol Cell Res*. 1866:1092–1100.

Tovey, S.C., De Smet, P., Lipp, P., Thomas, D., Young, K.W., Missiaen, L., De Smedt, H., Parys, J.B., Berridge, M.J., Thuring, J. and Holmes, A. 2001. Calcium puffs are generic $InsP_3$-activated elementary calcium signals and are downregulated by prolonged hormonal stimulation to inhibit cellular calcium responses. *J. Cell Sci*. 114:3979-3989.

Venkiteswaran, G. and Hasan, G. 2009. Intracellular Ca^{2+} signaling and store-

operated Ca^{2+} entry are required in *Drosophila* neurons for flight. *Proc. Natl. Acad. Sci. U. S. A.* 106:10326–10331.

Wojcikiewicz, R. J. H. 1995. Type I, II, and III inositol 1,4,5-trisphosphate receptors are unequally susceptible to down-regulation and are expressed in markedly different proportions in different cell types. *J. Biol. Chem*. 270:11678–11683.

Woo, J.S., Sun, Z., Srikanth, S. and Gwack, Y. 2020. The short isoform of extended synaptotagmin-2 controls Ca^{2+} dynamics in T cells via interaction with STIM1. *Sci. Rep*. 10:1-13.

Woodard, G.E., López, J.J., Jardín, I., Salido, G.M. and Rosado, J.A. 2010. TRPC3 regulates agonist-stimulated Ca^{2+} mobilization by mediating the interaction between type I inositol 1, 4, 5-trisphosphate receptor, RACK1, and Orai1. *J. Biol. Chem*. 285: 8045–8053.

Yoshikawa, F., Morita, M., Monkawa, T., Michikawa, T., Furuichi, T. and Mikoshiba, K. 1996. Mutational analysis of the ligand binding site of the inositol 1, 4, 5-trisphosphate receptor. *J. Biol. Chem.* 271:18277-18284.

Yue, L., Wang, L., Du, Y., Zhang, W., Hamada, K., Matsumoto, Y., Jin, X., Zhou, Y., Mikoshiba, K., Gill, D.L. and Han, S. 2020. Type 3 inositol 1, 4, 5-trisphosphate receptor is a crucial regulator of calcium dynamics mediated by endoplasmic reticulum in HEK cells. *Cells*. 9:275.

Figure 1. Loss of IP_3R1 Attenuates SOCE in Human Neural Stem Cells

(**A**) Confocal images of hNPCs (passage 6) stained for DAPI and neural stem cell proteins: Pax6 and Ki67 (proliferation marker). Scale bars, 50 µm.

(**B**) WB for IP_3R1 of hNPCs expressing non-silencing (NS) or IP_3R1-shRNA.

(**C**) Summary results (mean ± s.d., n = 3) show IP_3R1 expression relative to actin. $^{**}P < 0.01$, Student's t-test with unequal variances.

(**D**) Changes in $[Ca^{2+}]_c$ evoked by thapsigargin (Tg, 10 µM) in Ca^{2+}-free HBSS and then restoration of extracellular Ca^{2+} (2 mM) in hNPCs expressing NS or IP_3R1-shRNA. Mean ± s.e.m. from 3 independent experiments, each with 4 replicates that together included 100-254 cells. Inset shows the target of Tg.

(**E-G**) Summary results (individual cells, median (bar), 25th and 75th percentiles (box) and mean (circle)) show Ca^{2+} signals evoked by Tg or Ca^{2+} restoration (**E**), rate of Ca^{2+} entry (**F**) and resting $[Ca^{2+}]_c$ (**G**). $^{***}P < 0.001$, Mann-Whitney U-test.

(**H**) Changes in $[Ca^{2+}]_c$ evoked by Tg (10 µM) in Ca^{2+}-free HBSS and after restoring extracellular Ca^{2+} (2 mM) in neurons (differentiated hNPCs) expressing NS or IP_3R1-shRNA. Mean ± s.e.m. from 3 experiments with ~200 cells.

(**I,J**) Summary results (presented as in E-G) show Ca^{2+} signals evoked by Tg or Ca^{2+} restoration (**I**) and rate of Ca^{2+} entry (**J**). $^{***}P < 0.001$. Mann-Whitney U-test.

See also **Figure 1 - figure supplement 1.**

Source data in Figure 1 source data file

Figure 2. Loss of IP_3R1 Attenuates SOCE in SH-SY5Y Cells

(**A**) WB for IP_3R1-3 of SH-SY5Y cells expressing non-silencing (NS) or IP_3R1-shRNA.

(**B**) Summary results (mean ± s.d., n = 4) show IP_3R expression relative to actin normalized to control NS cells. $^{**}P < 0.01$, Student's t-test with unequal variances.

(**C**) Ca^{2+} signals evoked by carbachol (CCh, 3 µM) in SH-SY5Y cells expressing NS or IP_3R1-shRNA. Mean ± s.e.m. from 3 experiments with 70-90 cells.

(**D**) Summary results show peak changes in $[Ca^{2+}]_c$ ($\Delta[Ca^{2+}]_c$) evoked by CCh. $^{***}P < 0.001$, Mann-Whitney U-test.

(**E**) Ca^{2+} signals evoked by thapsigargin (Tg, 10 µM) in Ca^{2+}-free HBSS and then after restoration of extracellular Ca^{2+} (2 mM) in cells expressing NS or IP_3R1-shRNA. Mean ± s.e.m. from 3 experiments with ~50 cells.

(**F, G**) Summary results (individual cells, mean ± s.e.m., n = 3, ~50 cells) show peak changes in $[Ca^{2+}]_c$ evoked by Ca^{2+} restoration ($\Delta[Ca^{2+}]_c$) (**F**) and rate of Ca^{2+} entry (**G**). $^{***}P < 0.001$, Mann-Whitney U-test.

(**H**) Ca^{2+} signals evoked by Tg and then Ca^{2+} restoration in cells expressing NS-shRNA, or IP_3R1-shRNA alone or with IP_3R1 or IP_3R3. Traces show mean ± s.e.m. (50-115 cells from 3 experiments).

(**I, J**) Summary results (mean ± s.e.m, 50-115 cells from 3 experiments) show peak increases in $[Ca^{2+}]_c$ ($\Delta[Ca^{2+}]_c$) evoked by Ca^{2+} restoration (**I**) and rates of Ca^{2+} entry (**J**) evoked by restoring extracellular Ca^{2+}.

(**K**) Effects of thapsigargin (Tg, 10 µM) in Ca^{2+}-free HBSS and then after Ca^{2+} restoration (2 mM) in cells expressing IP_3R1-shRNA alone or with IP_3R1 or mCh-STIM1. Traces show mean ± s.e.m. (100-150 cells from 3 experiments).

(**L, M**) Summary results (mean ± s.e.m.) show peak increase in $[Ca^{2+}]_c$ after Ca^{2+} restoration ($\Delta[Ca^{2+}]_c$) (**L**) and rate of Ca^{2+} entry (**M**). Different letters indicate significant differences (panels I, J, L, M), $P < 0.001$, one-way ANOVA with pair-wise Tukey's test.

See also **Figure 2 with 3 supplements (Figure 2 - figure supplements 1 - 3).**

Source data in Figure 2 source data file

Figure 3. Regulation of SOCE by IP_3R Requires IP_3 Binding but Not a Functional Pore in SH-SY5Y cells

(**A**) SOCE is activated when loss of Ca^{2+} from the ER through IP_3Rs activates STIM1 (i). Our results suggest an additional role for IP_3Rs (ii).

(**B**) SH-SY5Y cells expressing IP_3R1-shRNA alone or with IP_3R1 or IP_3R1^{DA} were stimulated with thapsigargin (Tg, 1 µM) in Ca^{2+}-free HBSS before restoring extracellular Ca^{2+} (2 mM). Traces show mean ± s.e.m, for 100-150 cells from 3 experiments.

(**C**) Cells expressing IP_3R1-shRNA and IP_3R1^{DA} were treated with NS-siRNA or Orai1-siRNA before measuring Tg-evoked Ca^{2+} entry. Traces show mean ± s.e.m. for 85-100 cells from 3 experiments.

(**D**) Summary results (mean ± s.e.m.) show peak increases in $[Ca^{2+}]_c$ ($\Delta[Ca^{2+}]_c$) evoked by Ca^{2+} restoration.

(**E**) Tg-evoked Ca^{2+} entry in cells expressing IP_3R1-shRNA with IP_3R1, IP_3R1^{RQ} or $IP_3R1^{RQ/KQ}$. Traces show mean ± s.e.m, for 90-150 cells from 3 experiments.

(**F**) Summary results (mean ± s.e.m.) show peak increases in $[Ca^{2+}]_c$ ($\Delta[Ca^{2+}]_c$) evoked by Ca^{2+} restoration. Different letter codes (panels D, F) indicate significantly different values, $P < 0.001$, one-way ANOVA and pair-wise Tukey's test.

See also **Figure S3 - figure supplement 1.**

Source data in Figure 3 source data file

Figure 4. Receptor-Regulated IP_3 Production Stimulates SOCE in Cells With Empty Ca^{2+} Stores and Expressing Pore-Dead IP_3R

(**A, B**) SH-SY5Y cells expressing IP_3R1-shRNA alone (**A**) or with IP_3R1^{DA} (**B**) were treated with a low concentration of CPA (2 µM) in Ca^{2+}-free HBSS to partially deplete the ER of Ca^{2+} and sub-maximally activate SOCE (see **Figures S5M and S5N**). Carbachol (CCh, 1 µM) was then added to stimulate IP_3 formation through muscarinic receptors, and extracellular Ca^{2+} (2 mM) was then restored. Traces (mean ± s.e.m of 68-130 cells from 3 experiments) show responses with and without the CCh addition.

(**C**) Summary results show the peak increases in $[Ca^{2+}]_c$ ($\Delta[Ca^{2+}]_c$) after addition of CCh (CCh-induced Ca^{2+} release) and then after restoring extracellular Ca^{2+} (SOCE).

(**D-F**) SH-SY5Y cells wild type (WT) (**D**) and expressing NS-shRNA (**E**) or IP_3R1-shRNA (**F**) were treated with YM-254890 (YM, 1 µM, 5 min) in Ca^{2+}-free HBSS to inhibit Gαq and then with thapsigargin (Tg, 1 µM) before restoring extracellular Ca^{2+} (2 mM). Traces show mean ± s.e.m of ~120 cells from 3 experiments. .

(**G-I**) Similar analyses of HEK cells. Summary results (mean ± s.e.m, 50-100 cells from 3 experiments) are shown in (I).

Different letter codes (panels C and I) indicate significantly different values within the store Ca^{2+} release or SOCE groups, $P < 0.001$, one-way ANOVA and pair-wise Tukey's test.

See also **Figure 4 - figure supplement 1.**

Source data in Figure 4 source data file

Figure 5. IP_3Rs Promote Interaction of STIM1 With Orai1

(**A-E**) PLA analyses of interactions between STIM1 and Orai1 in SH-SY5Y cells expressing NS-shRNA (**A**) or IP_3R1-shRNA alone (**B**) or with IP_3R1 (**C**), IP_3R1^{DA} (**D**) or $IP_3R1^{RQ/KQ}$ (**E**). Confocal images are shown for control cells or after treatment with thapsigargin (Tg, 1 µM) in Ca^{2+}-free HBSS. PLA reaction product is red, and nuclei are stained with DAPI (blue). Scale bars, 5 µm. Summary results show the surface area of the PLA spots for 8-10 cells from 2 independent analyses. Individual values, median (bar) and 25th and 75th percentiles (box). $^{***}P < 0.001$, Student's *t*-test with unequal variances.

See also **Figure 5 - figure supplement 1.**

Source data in Figure 5 source data file

Figure 6. Extended Synaptotagmins Rescue SOCE in Cells Lacking IP_3R1

(**A**) SH-SY5Y cells expressing IP_3R1-shRNA alone or with E-Syt1 were stimulated with Tg (1 µM) in Ca^{2+}-free HBSS before restoring extracellular Ca^{2+} (2 mM). Traces show mean ± s.e.m, for 20-80 cells from 3 experiments.

(**B**) Summary results show $\Delta[Ca^{2+}]_c$ evoked by restoring Ca^{2+} (SOCE). Mean ± s.e.m, $^{***}P < 0.001$, Mann-Whitney U- test.

(**C**) Summary results (mean ± s.e.m, n = 20-80 cells) show resting $[Ca^{2+}]_c$ (left) and the peak Ca^{2+} signals ($\Delta[Ca^{2+}]_c$) evoked by thapsigargin (Tg, 1 µM) in Ca^{2+}-free HBSS for SH-SY5Y cells expressing IP_3R1-shRNA alone or with human E-Syt1.

(**D**) Cells over-expressing E-Syt1 and treated with IP_3R1-shRNA in combination with either NS or STIM1 siRNA were stimulated with Tg (1 µM) in Ca^{2+}-free HBSS before restoration of extracellular Ca^{2+} (2 mM). Mean ± s.e.m. from 3 experiments with 30-40 cells.

(**E, F**) Summary results (mean ± s.e.m, n = 30-40 cells) show SOCE evoked by Tg (**E**), resting $[Ca^{2+}]_c$ and the Tg-evoked Ca^{2+} release from intracellular stores (F). $^{***}P < 0.001$, one-way ANOVA with pair-wise Tukey's test.

(**G**) Similar analyses of cells expressing NS shRNA alone or with human E-Syt1 and then treated with Tg (1 µM) in Ca^{2+}-free HBSS before restoring extracellular Ca^{2+} (2 mM). Mean ± s.e.m. from 3 experiments with 115-135 cells.

(**H, I**) Summary results (mean ± s.e.m, n = 115-135 cells) show resting $[Ca^{2+}]_c$ (**H**) and $\Delta[Ca^{2+}]_c$ evoked by Tg (store release) or Ca^{2+} restoration (SOCE) (**I**). No significant difference, one-way ANOVA with pair-wise Tukey's test.

Source data in Figure 6 source data file

Figure 7. Dual Regulation of SOCE by IP_3Rs

(**A**) SOCE is activated when loss of Ca^{2+} from the ER, usually mediated by opening of IP_3Rs when they bind IP_3, causes STIM to unfurl cytosolic domains (2). The exposed cytosolic domains of STIM1 reach across a narrow gap between the ER and PM at a MCS to interact with PIP_2 and Orai1 in the PM. Binding of STIM1 to Orai1 causes pore opening, and SOCE then occurs through the open Orai1 channel. We show that IP_3Rs when they bind IP_3 also facilitate interactions between Orai1 and STIM, perhaps by stabilizing the MCS (1). Receptors that stimulate IP_3 formation thereby promote both activation of STIM (by emptying Ca^{2+} stores) and independently promote interaction of active STIM1 with Orai1.

(**B**) Other mechanisms, including ryanodine receptors (RyR), can also release Ca^{2+} from the ER. We suggest that convergent regulation of SOCE by IP_3R with bound IP_3 allows receptors that stimulate IP_3 formation to selectively control SOCE.

Figure 1 - figure supplement 1

Loss of IP_3R1 Attenuates SOCE In Neural Precursor Cells and Differentiated Neurons.

(**A-C**) hNPCs expressing NS (**A, C**) or IP_3R1-shRNA (**B**) were stimulated with carbachol (CCh, 100 µM) in Ca^{2+}-free HBSS before restoring extracellular Ca^{2+} (10 mM). Each trace shows the Fura 2 fluorescence ratio (F_{340}/F_{380}) from a single cell (>50 cells from 3 experiments). Traces in (**C**) show only cells that responded to CCh.

(**D, E**) hNPCs expressing shRNA were stimulated with thapsigargin (Tg, 10 µM) in Ca^{2+}-free HBSS before restoring extracellular Ca^{2+} (2 mM). Traces are from individual cells (>180 cells from 3 experiments), with the mean response shown by a thick line. Summary results in **Figures 1D-1G.**

(**F**) Confocal images of hNPCs and neurons spontaneously differentiated (10 days) from hNPCs stained for DAPI and neuronal markers: Tuj1 (βIII-tubulin) and NeuN (neuronal nuclear antigen). Scale bars, 50 µm. Only differentiated hNPCs express neuronal markers.

(**G**) WB for STIM1 and Orai1 in lysates from hNPCs cells expressing non-silencing (NS) or IP_3R1-shRNA. Summary results (mean ± s.d., n = 3) show relative expression of STIM1 and Orai1 relative to control shRNA (NS) cells. $P > 0.01$, Student's *t*-test with unequal variances.

(**H, I**) Spontaneously differentiated hNPCs (25 days) expressing NS (**H**) or IP_3R1-shRNA (**I**) were depolarized by addition of KCl (75 mM). Traces show responses from single cells (>30 cells from 3 experiments) and mean response (thick line).

(**J**) Summary results (mean ± s.e.m., 3 experiments) show peak increases in $[Ca^{2+}]_c$ ($\Delta[Ca^{2+}]_c$) evoked by depolarization. No significant difference, Student's *t*-test with unequal variances.

(**K, L**) Spontaneously differentiated hNPCs expressing NS (**K**) or IP_3R1-shRNA (**L**) were stimulated with Tg (10 µM) in Ca^{2+}-free HBSS before restoring extracellular Ca^{2+} (2 mM). Traces from individual cells (>100 cells from 3 experiments) and the mean response (bold) are shown. Summary results in **Figure 1H-1J.**

Source data in Figure 1 - figure supplement 1 source data file.

Figure 2 - figure supplement 1

Reduced Expression of IP_3R1 Using either shRNA or CRISPR/Cas9n Attenuates SOCE in SH-SY5Y Cells

(**A, B**) Ca^{2+} signals evoked by carbachol (CCh, 3 μM) in Ca^{2+}-free HBSS in SH-SY5Y cells expressing NS (**A**) or IP_3R1-shRNA (**B**). Traces show responses from single cells (100-200 cells from 3 experiments).

(**C, D**) SH-SY5Y cells expressing NS (**C**) or IP_3R1-shRNA (**D**) were treated with thapsigargin (Tg, 1 μM) in Ca^{2+}-free HBSS before restoration of extracellular Ca^{2+} (2 mM). Traces show responses from single cells (50-100 cells from 3 experiments) and mean response (thick lines). Summary results in **Figures 2C-2G**.

(**E**) Western blots (WB) for STIM1 and Orai1 from lysates of SH-SY5Y cells expressing non-silencing (NS) or IP_3R1-shRNA. Summary results (mean ± s.d., n = 3) show STIM1 and Orai1 expression relative to NS-shRNA cells. $P > 0.05$, Student's *t*-test with unequal variances.

(**F**) Western blot for IP_3R1 and tubulin from lysates from WT SH-SY5Y cells and for cells from a cell line in which the IP_3R1 gene was targeted using CRISPR/Cas9 (IKO null). The blot is typical of 3 similar analyses. Summary results (mean ± s.d., n = 3) show IP_3R1 expression relative to WT cells. $P < 0.001$, Student's *t*-test with unequal variances.

(**G**) Western blots (WB) for STIM1 (S1), STIM2 (S2) and Orai1 (O1) from lysates of WT and IKO null SH-SY5Y cells. Summary results (mean ± s.d., n = 3) show STIM1,2 and Orai1 expression relative to WT cells. $P > 0.05$, Student's t-test with unequal variances.

(**H**) Ca^{2+} signals evoked by carbachol (CCh, 1 μM) in WT and IKO null SH-SY5Y cells in Ca^{2+}-free HBSS.

(**I**) SH-SY5Y cells (WT or IKO null) were treated with thapsigargin (Tg, 1 μM) in Ca^{2+}-free HBSS before restoring extracellular Ca^{2+} (2 mM). Mean ± s.e.m. from 3 experiments with WT cells (black, 110 cells), IKO null cells (red, 117 cells).

(**J**) Summary results show the peak increases in $[Ca^{2+}]_c$ evoked by Tg (1 μM) in Ca^{2+}-free HBSS ($\Delta[Ca^{2+}]_c$) and after Ca^{2+} restoration (SOCE). Different letters indicate P < 0.001, Mann-Whitney U-test.

(**K**) PCRs for IP_3R1 and GAPDH (control gene) of genomic DNA isolated from SH-SY5Y cells. Results (mean ± s.e.m. from 3 independent analyses of a single cell line) are shown for wild type (WT) cells and for cells in which the IP_3R1 gene was targeted using CRISPR/Cas9n (IKO). Expression of IP_3R1 has been normalized to expression of GAPDH. $^{**}P < 0.01$, Student's *t*-test with unequal variances.

(**L**) Droplet digital PCR amplification was used to determine gene copy number for IP_3R1 and a control gene RPP30 for WT and IKO SH-SY5Y cells. $^{**}P < 0.05$, Student's *t*-test with unequal variances.

(M) Western blot for IP_3R1 and tubulin from lysates from WT SH-SY5Y cells and for cells from a cell line in which the IP_3R1 gene was targeted using CRISPR/Cas9n (IKO). The blot is typical of 3 similar analyses. Summary results (mean ± s.d., n = 3) show IP_3R1 expression relative to WT cells. P < 0.01, Student's *t*-test with unequal variances.

(**N**) Ca^{2+} signals evoked by carbachol (CCh, 1 μM) in WT and IKO SH-SY5Y cells in Ca^{2+}-free HBSS. Results show (mean ± s.e.m.) for each of three independently edited

cell lines (IKO1, 2 and 3), each with at least 30 cells; and the overall mean ± s.e.m. (red line). Results from a total of 89 WT cells and 130 IKO cells are shown.

(**O**) Summary results (mean ± s.e.m. from 3 experiments with 80-100 cells) show peak changes in $[Ca^{2+}]_c$ ($\Delta[Ca^{2+}]_c$) evoked by CCh. ****P* < 0.001, Mann-Whitney U-test.

(**P**) SH-SY5Y cells (WT or IKO) were treated with thapsigargin (Tg, 1 µM) in Ca^{2+}-free HBSS before restoring extracellular Ca^{2+} (2 mM). Mean ± s.e.m. from 3 experiments with WT cells (black, 85 cells), 3 independently edited cell lines (IKO 1, 2 and 3; at least 30 cells for each) and the pooled results from all edited cells (97; red).

(**Q**) Summary results show the peak increases in $[Ca^{2+}]_c$ evoked by Tg (1 µM) in Ca^{2+}-free HBSS ($\Delta[Ca^{2+}]_c$) and after Ca^{2+} restoration (SOCE). Different letters indicate P < 0.001, Mann-Whitney U-test.

Source data in Figure 2 - figure supplement 1 source data file.

Figure 2 - figure supplement 2

Attenuated SOCE In SH-SY5Y Cells Lacking IP_3R1 is Rescued by Expression of IP_3R1, IP_3R3 or STIM1.

(**A**) Ca^{2+} signals evoked by carbachol (CCh, 3 µM) in SH-SY5Y cells expressing NS or IP_3R1-shRNA, and the latter with IP_3R1 or IP_3R3. Traces show mean ± s.e.m. from >3 experiments with 50-70 cells.

(**B-D**) Summary results show peak Ca^{2+} signals ($\Delta[Ca^{2+}]_c$) evoked by CCh (**B**), resting $[Ca^{2+}]_c$ (**C**) and the peak Ca^{2+} signal evoked by Tg (10 µM) in Ca^{2+}-free HBSS ($\Delta[Ca^{2+}]_c$, a reporter of ER Ca^{2+} content) (**D**). Different letter codes indicate significantly different values, $P < 0.001$, one-way ANOVA and pair-wise Tukey's test.

(**E**) Effects of expressing mCh-STIM1 in SH-SY5Y cells expressing NS shRNA on the Ca^{2+} signals evoked by Tg (1 µM) in Ca^{2+}-free HBSS and then after restoration of extracellular Ca^{2+} (2 mM). Traces show mean ± s.e.m. from 3 experiments with 30-110 cells.

(**F**) Summary results show the peak $\Delta[Ca^{2+}]_c$ evoked by restoring extracellular Ca^{2+} after Tg. Mean ± s.e.m. $P > 0.05$, Mann-Whitney U-test.

Source data in Figure 2 - figure supplement 2 source data file.

Figure 2 - figure supplement 3

Loss of IP_3R1 Does Not affect SOCE in HEK Cells.

(**A**) WB for IP_3R1 in HEK cells expressing non-silencing (NS) or IP_3R1-shRNA. Summary results (mean ± s.d., n = 3) show IP_3R1 expression relative to tubulin. $^{***}P <$ 0.001, Student's *t*-test with unequal variances.

(**B**) HEK cells expressing NS or IP_3R1-shRNA were treated with thapsigargin (Tg, 1 µM) in Ca^{2+}-free HBSS before restoration of extracellular Ca^{2+} (2 mM). Traces show mean response from >100 cells from 3 experiments.

(**C**) Summary results show the peak increases in $[Ca^{2+}]_c$ evoked by Tg (1 µM) in Ca^{2+}-free HBSS ($\Delta[Ca^{2+}]_c$, a reporter of ER Ca^{2+} content) and after Ca^{2+} restoration (SOCE).

(**D**) Wild type HEK cells (HEK WT) and cells lacking all IP_3Rs (HEK-TKO) were treated with thapsigargin (Tg, 1 µM) in Ca^{2+}-free HBSS before restoration of extracellular Ca^{2+} (2 mM). Traces show mean ± s.e.m. from 3 experiments with 80-120 cells.

(**E**) Summary results show the peak $\Delta[Ca^{2+}]_c$ evoked by restoring extracellular Ca^{2+} after Tg. Mean ± s.e.m. $P > 0.01$, Mann-Whitney U-test.

(**F**) Proximity ligation assay (PLA) analyses of interactions between STIM1 and Orai1 in wild type HEK (WT) and TKO cells. Confocal images are shown for control cells (-Tg) or after treatment with thapsigargin (+Tg, 1 µM) in Ca^{2+}-free HBSS. PLA reaction product is red, and nuclei are stained with DAPI (blue). Scale bars, 5 µm. Summary results show the surface area of the PLA spots for ~20 cells from 2 independent analyses. Individual values, median (bar) and 25th and 75th percentiles (box). ***P < 0.01, Student's t-test with unequal variances.

Source data in Figure 2 - figure supplement 3 source data file.

Figure 3 - figure supplement 1

Attenuated SOCE In SH-SY5Y Cells Lacking IP_3R1 is Rescued by Expression of Pore-Dead IP_3R1 with a Functional IP_3-Binding Site.

(**A**) WB with IP_3R1 antibody showing expression of IP_3R1 and IP_3R1^{DA} in SH-SY5Y cells expressing IP_3R1-shRNA.

(**B**) Summary (mean ± s.e.m, n = 3) shows IP_3R1 expression normalized to actin. $P < 0.001$, one-way ANOVA with pair-wise Tukey's test. Here, and in most subsequent panels, different letters indicate groups that are statistically different, with the test defined for each panel.

(**C**) Ca^{2+} signals evoked by carbachol (CCh 3 μM) in SH-SY5Y cells expressing IP_3R1-shRNA alone or with IP_3R1, IP_3R1^{DA}, $IP_3R1^{RQ/KQ}$ or IP_3R1^{1-604}. Traces show mean ± s.e.m. from 3 experiments.

(**D**) Summary results (mean ± s.e.m) show peak changes in $[Ca^{2+}]_c$ evoked by CCh ($\Delta[Ca^{2+}]_c$). $P < 0.001$, one-way ANOVA with pair-wise Tukey's test.

(**E**) Resting $[Ca^{2+}]_c$ (left) and thapsigargin (Tg)-evoked Ca^{2+} release (1 μM, $\Delta[Ca^{2+}]_c$) (right) in cells treated as indicated. $P < 0.001$, one-way ANOVA with pair-wise Tukey's test.

(**F**) WB showing Orai1 expression in cells expressing IP_3R1-shRNA and IP_3R1^{DA}, and then treated with NS or Orai1-siRNA.

(**G**) Summary results (normalized to GAPDH expression, mean ± s.d, n =3). $^{**}P < 0.01$, Student's t-test with unequal variances.

825 (**H**) Resting $[Ca^{2+}]_c$ (left) and Tg-evoked Ca^{2+} release (right) in cells expressing IP_3R1-
826 shRNA and IP_3R1^{DA}, and then treated with NS or Orai1-siRNA. $P < 0.05$, Mann-
827 Whitney U-test.
828 (**I**) WB for IP_3R1 in cells expressing IP_3R1-shRNA alone or with IP_3R1 or $IP_3R1^{RQ/KQ}$.
829 Results typical of 2 independent experiments.
830 (**J**) Resting $[Ca^{2+}]_c$ (left) and Ca^{2+} release evoked by Tg (right) in cells expressing
831 IP_3R1-shRNA alone or with the indicated IP_3R1. Mean ± s.e.m., $n = 3$ experiments. P
832 < 0.001, one-way ANOVA with pair-wise Tukey's test.
833 (**K**) Changes in $[Ca^{2+}]_c$ evoked by Tg (10 µM) in Ca^{2+}-free HBSS and then after
834 restoration of extracellular Ca^{2+} (2 mM) in cells expressing IP_3R1-shRNA alone or with
835 IP_3R1 or IP_3R1^{1-604}. Mean ± s.e.m. from 3 experiments with >100 cells.
836 **(L**) Summary results show peak increases in $[Ca^{2+}]_c$ evoked by Ca^{2+} restoration in the
837 indicated cells. $P < 0.001$, one-way ANOVA with pair-wise Tukey's test.
838 (**M**) SH-SY5Y cells expressing NS-shRNA were stimulated with the indicated
839 concentrations of CPA in Ca^{2+}-free HBSS to partially deplete ER Ca^{2+} stores and then
840 with ionomycin (Iono, 1 µM) to release all remaining Ca^{2+}. Results show mean ±
841 s.e.m. for >30 cells from 3 experiments.
842 (**N**) Summary results (mean ± s.e.m.) show $\Delta[Ca^{2+}]_c$ evoked by CPA or ionomycin. $P <$
843 0.001, one-way ANOVA with pair-wise Tukey's test. The results confirm that the lower
844 concentrations of CPA partially deplete the ER of Ca^{2+}.
845 **(O**) Summary results (mean ± s.e.m, 80-100 cells from 3 experiments) show the peak
846 increases in $[Ca^{2+}]_c$ ($\Delta[Ca^{2+}]_c$) after adding Tg (store Ca^{2+} release) and after restoring
847 extracellular Ca^{2+} (SOCE) with or without YM-254890 treatment. Different letter codes

indicate significantly different values within the Ca^{2+} release or SOCE groups, $P <$ 0.001, one-way ANOVA and pair-wise Tukey's test.

Source data in Figure 3 - figure supplement 1 source data file.

Figure 4 - figure supplement 1

Effects of Inhibiting Gq on Ca^{2+} Signals and STIM1-Orai1 interactions in SH-SY5Y and HEK Cells.

(**A**) PLA analyses of interactions between STIM1 and Orai1 in wild type (WT) SH-SY5Y cells untreated (-YM) or treated (+YM, 1µm) with Gq inhibitor YM-254890. Confocal images are shown for control cells (-Tg) or after treatment with thapsigargin (+Tg, 1 µM) in Ca^{2+}-free HBSS. PLA reaction product is red, and nuclei are stained with DAPI (blue). Scale bars, 5 µm. Summary results show the surface area of the PLA spots for ~20 cells from 2 independent analyses. Individual values, median (bar) and 25th and 75th percentiles (box). ***P < 0.01, Student's t-test with unequal variances.

(**B**) HEK cells expressing NS shRNA and treated with the Gq inhibitor, YM-254890 (YM, 1 µM, 5 min) were stimulated with carbachol (CCh, 100 µM). Traces show mean ± s.e.m. from 3 experiments with 30-40 cells. The results confirm that treatment with YM-254890 effectively uncouples CCh from IP_3-evoked Ca^{2+} signals.

(**C**) From results shown in **Figures 4G and 4H**, rates of thapsigargin-evoked Ca^{2+} entry were determined. Summary shows mean ± s.e.m, from 100-120 cells. $P < 0.001$, Mann-Whitney U-test.

(**D-E**) Changes in $[Ca^{2+}]_c$ evoked by thapsigargin (Tg, 1 µM) in Ca^{2+}-free HBSS and then after restoration of extracellular Ca^{2+} (2 mM) in WT (**C**) and TKO (**D**) HEK cells after treatment with YM-254890 (YM, 1 µM, 5 min). Traces show mean ± s.e.m. from 3 experiments with 100-120 cells.

(**F**) Summary results show peak increase in $[Ca^{2+}]_c$ ($\Delta[Ca^{2+}]_c$) evoked by addition of thapsigargin and then after restoring extracellular Ca^{2+} (SOCE). Mean ± s.e.m. Different letter codes (C and G) indicate significantly different values, $P < 0.001$, one-way ANOVA and pair-wise Tukey's test.

Source data in Figure 4 - figure supplement 1 source data file.

Figure 5 - figure supplement 1

Validation of PLA Measurements of Orai1-STIM1 Interactions.

(**A**) PLA using antibodies to Orai1 and STIM1 to establish whether they are associated. Complementary oligonucleotides conjugated to a secondary antibody (2nd) targeting their respective primary antibodies (1st) hybridize when they are close to each other, allowing rolling circle amplification (RCA) and production of a red fluorescent product. The latter can be quantified from the surface area of the fluorescent spots or their intensity. We obtained indistinguishable results with both methods of quantification. We therefore show only results obtained from surface-area measurements.

(**B-D**) Confocal images from PLA assays of SH-SY5Y cells expressing NS-shRNA performed with no primary antibody (**B**), or with primary antibody for only STIM1 (**C**) or only Orai1 (**D**). Scale bars, 5 µm.

(**E, F**) Confocal images of SH-SY5Y cells expressing NS-shRNA with (**F**) or without thapsigargin treatment (**E**) (Tg, 1 µM, in Ca^{2+}-free HBSS). Cells are stained with DAPI and immunostained for Orai1 or STIM1. Scale bars, 5 µm.

(G-N) Similar analyses of cells expressing IP_3R1-shRNA alone (**G, H**), or with IP_3R1 (**I, J**), IP_3R1^{DA} (**K, L**) or $IP_3R1^{RQ/KQ}$ (**M, N**). Results (**E-N**) are typical of 2 experiments. The PLA results are shown in **Figure 5**.

RESOURCE AVAILABILITY

Lead Contact

All requests for resources and reagents should be directed to the lead contact, Dr. Gaiti Hasan (gaiti@ncbs.res.in).

Materials Availability

Constructs and cell lines are available upon request. MTA required for cell lines.

Data and Code Availability

This study did not generate any computer code. The data supporting the findings of this study are available within the manuscript. All other data supporting the findings of this study are available in source data file of respective figures.

METHOD DETAILS

Culture of Human Neural Precursor Cells

Human neural precursor cells (hNPCS) were derived from a human embryonic stem cell (hESC) line, H9/WA09 (RRID: CVCL_9773), using a protocol that inhibits dual SMAD signalling and stimulates Wnt signaling (Reinhardt *et al.*, 2013) as described previously (Gopurappilly *et al.*, 2018, 2019). hNPCs were grown as adherent dispersed cells on growth factor-reduced Matrigel (0.5%, Corning, Cat#356230) in hNPC maintenance medium (NMM) at 37°C in humidified air with 5% CO_2. NMM comprised a 1:1 mixture of Dulbecco's Modified Eagle Medium with Nutrient Mixture F-12 (DMEM/F-12, Invitrogen, Cat#10565018) and Neurobasal medium

(ThermoFisher, Cat#21103049), supplemented with GlutaMAX (0.5x, ThermoFisher, Cat#35050061), N2 (1:200, ThermoFisher, 17502048), B27 without vitamin A (1:100, ThermoFisher, Cat#12587010), Antibiotic-Antimycotic (ThermoFisher, Cat#15240112), CHIR99021 (3 μM, STEMCELL Technologies, Cat#72052), purmorphamine (0.5 mM, STEMCELL Technologies, Cat#72202) and ascorbic acid (150 μM, Sigma, Cat#A92902). Doubling time was ~24 hr. Cells were passaged every 4-5 days by treatment with StemPro Accutase (ThermoFisher, Cat#A1110501), stored in liquid nitrogen, and thawed as required. Cells were confirmed to be mycoplasma-free by monthly screening (MycoAlert, Lonza, Cat#LT07-318). hNPCs between passages 16-19 were used.

All experiments performed with hESC lines were approved by the Institutional Committee for Stem Cell Research, registered under the National Apex Committee for Stem Cell Research and Therapy, Indian Council of Medical Research, Ministry of Health, New Delhi.

Stable Knockdown of IP_3R1

An UltramiR lentiviral inducible shRNA-mir based on the shERWOOD algorithm (Auyeung *et al.*, 2013; Knott *et al.*, 2014) was used to inhibit IP_3R1 expression. The all-in-one pZIP vector, which allows puromycin-selection and doxycycline-induced expression of both shRNA-mir and Zs-Green for visualization, was from TransOMIC Technologies (Huntsville, AL). Lentiviral pZIP transfer vectors encoding non-silencing shRNA (NS, NT#3-TTGGATGGGAAGTTCACCCCG) or IP_3R1-targeting shRNA (ULTRA3316782- TTTCTTGATCACTTCCACCAG) were packaged as lentiviral particles using packaging (pCMV- dR8.2 dpvr, Addgene, plasmid #8455) and

envelope vectors (pCMV-VSV-G, Addgene, plasmid #8454) by transfection of HEK293T cells (referred as HEK, ATCC, Cat# CRL-3216). Viral particles were collected and processed and hNPCs (passage 9) or SH-SY5Y cells were transduced (multiplicity of infection, MOI = 10) using Lipofectamine LTX with PLUS reagent (ThermoFisher, Cat#15338100). Cells were maintained in media containing doxycycline (2 µg/ml, Sigma, Cat# D3072) to induce shRNA expression, and puromycin to select transduced cells (1 µg/ml for hNPCs; 3 µg/ml for SH-SY5Y cells; Sigma, Cat# P9620). Cells were passaged 4-5 times after lentiviral transduction to select for stable expression of shRNAs.

Derivation of Neurons From hNPCs

Neurons were differentiated from hNPCs stably transduced with shRNA. hNPCs were seeded at 50-60% confluence in NMM on coverslips coated with poly-d-lysine (0.2 mg/ml, Sigma, Cat#P7280). After 1-2 days, the medium was replaced with neuronal differentiation medium, which comprised a 1:1 mixture of DMEM/F-12 with Neurobasal supplemented with B27 (1:100), N2 (1:200), GlutaMAX (0.5x) and Antibiotic-Antimycotic solution. Medium was replaced on alternate days. Neurons were used after 15-20 days.

Culture and Transfection of SH-SY5Y Cells

SH-SY5Y cells (ATCC, USA, Cat# CRL-2266) were grown on culture dishes in DMEM/F-12 with 10% fetal bovine serum (Sigma, Cat# F4135) at 37 °C in humidified air with 5% CO_2. Cells were passaged every 3-4 days using TrypLE Express (ThermoFisher, Cat# 12605036) and confirmed to be free of mycoplasma. Cells expressing shRNA were transiently transfected using TransIT-LT1 reagent (Mirus,

Cat# MIR-2300) in Opti-MEM (ThermoFisher, Cat# 31985062). Plasmids (250 ng) and/or siRNA (200 ng) in transfection reagent (1 µg/2.5 µl) were added to cells grown to 50% confluence on glass coverslips attached to an imaging dish. Cells were used after 48 hrs. The siRNAs used were to human Orai1 (100 nM, Dharmacon, Cat# L-014998-00-0005) or non-silencing (NS, Dharmacon, Cat# D-495 001810-10-05), to human STIM1 (Santa Cruz Biotechnology, Cat# sc-76589) or NS (Santa Cruz Biotechnology, Cat# sc-37007). The expression plasmids were IP_3R1 (rat type 1 IP_3R1 in pcDNA3.2/V5DEST vector) (Dellis *et al.*, 2008), rat IP_3R1^{DA} (D2550 replaced by A in pcDNA3.2 vector) (Dellis *et al.*, 2008), rat IP_3R1^{RQ} (R568 replaced by Q of type 1 IP_3R in pCDNA3.2/V5DEST vector) (Dellis *et al.*, 2008), rat $IP_3R1^{RQ/KQ}$ (R568 and K569 replaced by Q of type 1 IP_3R in pCDNA3.2/V5DEST vector), rat IP_3R1^{1-604} (residues 1-604 of IP_3R with N-terminal GST tag in pCDNA3.2/V5DEST vector) (Dellis *et al.*, 2008), rat IP_3R3 (rat type 3 IP_3R in pcDNA3.2/V5DEST vector) (Saleem *et al.*, 2013), human mCherry-STIM1 (N terminal mCherry tagged human STIM1 in pENTR1a vector) (Nunes-Hasler *et al.*, 2017) and human extended synaptotagmin 1 (E-Syt1), a kind gift from Dr S. Muallem, NIDCR, USA (Maléth *et al.*, 2014).

CRISPR/Cas9 and Cas9n Editing of SH-SY5Y Cells

To allow either CRISPR/Cas9 or Cas9n-mediated disruption of IP_3R1 expression, we used a published method to clone gRNAs into the backbone vector (pSpCas9n(BB)-2A-Puro PX462 V2.0, Addgene, Cat#62987) (Ran *et al.*, 2013). Forward and reverse sgRNA oligonucleotides (100 µM) were annealed and ligated using T4 DNA ligase by incubation (10 µl, 37°C, 30 min) before slow cooling to 20°C. Plasmids encoding Cas9n were digested with *BbsI-HF* (37°C, 12 hr), gel-purified (NucleoSpin Gel and

PCR Clean-up kit from Takara) and the purified fragment was stored at -20°C. A mixture (final volume 20 µl) of gRNA duplex (1 µl, 0.5 µM), digested px459 (for IKO null) or pX462 vector (for IKO) (30 ng), 10×□T4 DNA ligase buffer (2 µl) and T4 DNA ligase (1 µl) was incubated (20°C, 1 hr). After transformation of DH5-α competent *E. coli* with the ligation mixture, plasmids encoding Cas9 or Cas9n and the sgRNAs were extracted, and the coding sequences were confirmed (Ran *et al.*, 2013). The plasmid (2 µg) was then transfected into SH-SY5Y cells (50-60% confluent) in a 6-well plate using TransIT LT-1 reagent (Mirus Bio, Cat# MIR-2300). After 48 hr, puromycin (3 µg/ml, 72 hr) was added to kill non-transfected cells. IKO colonies were propagated and screened for Ca^{2+} signals evoked by carbachol and for the presence of the IP_3R gene by genomic DNA PCR and droplet digital PCR using primers close to the region targeted by the gRNAs (Miotke *et al.*, 2014). Three independently derived IKO lines, each with one residual IP_3R1 gene, were used for analyses of Ca^{2+} signaling (see **Figure S2N-S2Q**). For one of the cell lines (IKO 2), disruption of one copy of the IP_3R1 gene was confirmed by genomic PCR, droplet digital PCR and Western blotting (**Figures S2K-S2M**). For the IKO null line, single cell selection was done in a 96 well plate setup followed by screening for carbachol-evoked Ca^{2+} signals from multiple clones. A single clone was selected (**Figure S2H**) and a western blot performed to confirm absence of IP_3R1 expression (**Figure S2F**). All the oligonucleotide sequences are described in **supplementary file 1.**

Ca^{2+} Imaging

Methods for single-cell Ca^{2+} imaging were described previously (Gopurappilly *et al.*, 2019)**.** Briefly, cells grown as a monolayer (~70% confluence) on homemade

coverslip-bottomed dishes were washed and loaded with Fura 2 by incubation with Fura 2 AM (4 μM, 45 min, 37°C, ThermoFisher, Cat# F1221), washed and imaged at room temperature in HEPES-buffered saline solution (HBSS). HBSS comprised: 20 mM HEPES, 137 mM NaCl, 5 mM KCl, 2 mM $MgCl_2$, 2 mM $CaCl_2$, 10 mM glucose, pH 7.3. $CaCl_2$ was omitted from Ca^{2+}-free HBSS. Treatments with carbachol (CCh, Sigma, Cat# C4382), thapsigargin (Tg, ThermoFisher, Cat# 7458), cyclopiazonic acid (CPA, Sigma Cat# C1530) or high-K^+ HBSS (HBSS supplemented with 75 mM KCl) are described in legends.

Responses were recorded at 2-s intervals using an Olympus IX81-ZDC2 Focus Drift-Compensating Inverted Microscope with 60× oil immersion objective (numerical aperture, NA = 1.35) with excitation at 340 nm and 380 nm. Emitted light (505 nm) was collected with an Andor iXON 897E EMCCD camera and AndoriQ 2.4.2 imaging software (RRID: SCR_014461). Maximal (R_{max}) and minimal (R_{min}) fluorescence ratios were determined by addition of ionomycin (10 μM, Sigma, Cat# 407953) in HBSS containing 10 mM $CaCl_2$ or by addition of Ca^{2+}-free HBSS containing BAPTA (10 mM, Sigma, Cat# 196418) and Triton X100 (0.1%). Background-corrected fluorescence recorded from regions of interest ROI) drawn to include an entire cell was used to determine mean fluorescence ratios ($R = F_{340}/F_{380}$) (ImageJ), and calibrated to $[Ca^{2+}]_c$ from (Grynkiewicz, Poenie and Tsien, 1985):

$$[\mathrm{Ca}^{2+}]_c = K_D \cdot \frac{F_{380}^{min}}{F_{380}^{max}} \cdot \frac{(R - R_{min})}{(R_{max} - R)}$$

where, K_D = 225 nM (Forostyak *et al.*, 2013).

Western Blots

Proteins were isolated in RIPA buffer (Sigma, Cat# R0278) with protease inhibitor cocktail (Sigma, Cat# P8340) or, for WB of Orai1, in medium containing 150 mM NaCl, 50 mM Tris, 1% Triton-X-100, 0.1% SDS and protease inhibitor cocktail. After 30 min on ice with intermittent shaking, samples were collected by centrifugation (11,000 ×*g*, 20 min) and their protein content was determined (Thermo Pierce BCA Protein Assay kit, ThermoFisher, Cat# 23225). Proteins (~30 µg/lane) were separated on 8% SDS-PAGE gels for IP_3R or 10% SDS-PAGE gels for STIM1 and Orai1, and transferred to a Protran 0.45-µm nitrocellulose membrane (Merck, Cat# GE10600003) using a TransBlot semi-dry transfer system (BioRad, Cat# 1703940). Membranes were blocked by incubation (1 hr, 20°C) in TBST containing skimmed milk or bovine serum albumin (5%, Sigma, Cat# A9418). TBST (Tris-buffered saline with Tween) comprised: 137 mM NaCl, 20 mM Tris, 0.1% Tween-20, pH 7.5. Membranes were incubated with primary antibody in TBST (16 hr, 4°C), washed with TBST (3□×10 min), incubated (1 hr, 20°C) in TBST containing HRP-conjugated secondary antibody (1:3000 anti-mouse, Cell Signaling Technology Cat# 7076S; or 1:5000 anti-rabbit, ThermoScientific Cat# 32260). After 3 washes, HRP was detected using Pierce ECL Western Blotting Substrate (ThermoFisher, Cat# 32106) and quantified using ImageQuant LAS 4000 (GE Healthcare) and Image J. The primary antibodies used were to: IP_3R1 (1:1000, ThermoFisher, Cat# PA1-901, RRID: AB_2129984); β-actin (1:5000, BD Biosciences, Cat# 612656, RRID: AB_2289199); STIM1 (1:1000, Cell Signaling Technology, Cat# 5668S, RRID: AB_10828699); Orai1 (1:500, ProSci, Cat# PM-5205, RRID: AB_10941192); IP_3R2 (1:1000, custom made by Pocono Rabbit

Farm and Laboratory) (Mataragka and Taylor, 2018); and IP_3R3 (1:500, BD Biosciences, Cat# 610313, RRID: AB_397705).

Immunocytochemistry

After appropriate treatments, cells on a coverslip-bottomed plate were washed twice with cold PBS, fixed in PBS with paraformaldehyde (4%, 20°C, 20 min), washed (3 × 5 min) with PBS containing Triton-X100 (0.1%, PBST) and blocked by incubation (1 hr, 20°C) in PBST containing goat serum (5%). After incubation with primary antibody in PBST (16 hr, 4°C) and washing with PBST (3 × 5 min), cells were incubated (1 hr, 20°C) with secondary antibody in PBST containing goat serum, washed (3 × 5 min), stained (10 min, 20°C) with DAPI (1 µg/ml in PBS; Sigma, Cat# D9542) and washed (5 min, PBST). Cells were then covered with glycerol (60% v/v) and imaged using an Olympus FV300 confocal laser scanning microscope with 20× or 60× oil-immersion objectives. Fluorescence was analyzed using ImageJ. The primary antibodies used were to: PAX6 (1:500, Abcam, Cat# ab195045, RRID: AB_2750924); Nestin (1:500, Abcam, Cat# 92391, RRID: AB_10561437); Ki67 (1:250, Abcam, Cat# ab16667, RRID: AB_302459); SOX1 (1:1000, Abcam, Cat# ab87775, RRID: AB_2616563); Tuj1 (βIII Tubulin 1:1000, Promega, Cat# G712, RRID: AB_430874); NeuN (1:300, Abcam, Cat# ab177487, RRID: AB_2532109); Doublecortin (1:500, Abcam, Cat# 18723, RRID: AB_732011); MAP2 (1:200, Abcam, Cat# ab32454, RRID: AB_776174); STIM1 (1:1000, Cell Signaling Technology, Cat# 5668S, RRID: AB_10828699); and Orai1 (1:500, ProSci, Cat# PM-5205, RRID: AB_10941192).

Proximity Ligation Assay

The Duolink *In Situ* Red Starter Mouse/Rabbit kit was from Sigma (#Cat DUO92101) and used according to the manufacturer's protocol with primary antibodies to Orai1 (mouse 1:500) and STIM1 (rabbit 1:1000). Cells (~30% confluent) were treated with thapsigargin (1 μM, 5 min) in Ca^{2+}-free HBSS before fixation, permeabilization, and incubation with primary antibodies (16 hr, 4°C) and the PLA reactants. Red fluorescent PLA signals were imaged using an Olympus FV300 confocal laser scanning microscope, with excitation at 561 nm, and a 60× oil-immersion objective. Quantitative analysis of the intensity and surface area of PLA spots used the "Analyze particle" plugin of Fiji. Results are shown for 8-10 cells from two biological replicates of each genotype.

Statistical Analyses

All experiments were performed without blinding or prior power analyses. Independent biological replicates are reported as the number of experiments (n), with the number of cells contributing to each experiment indicated in legends. The limited availability of materials for PLA restricted the number of independent replicates (n) to 2 (each with 8-10 cells). Most plots show means ± s.e.m. (or s.d.). Box plots show 25th and 75th percentiles, median and mean (see legends). Where parametric analyses were justified by a Normality test, we used Student's *t*-test with unequal variances for 2-way comparisons and ANOVA followed by pair-wise Tukey's test for multiple comparisons. Non-parametric analyses used the Mann-Whitney U-test. Statistical significance is shown by $^{***}P < 0.001$, $^{**}P < 0.01$, $^{*}P < 0.05$, or by letter codes wherein different letters

indicate significantly different values ($P < 0.001$, details in legends). All analyses used Origin 8.5 software.

Details of the plasmids and recombinant DNAs are given in Supplementary file 1.

Figure 1

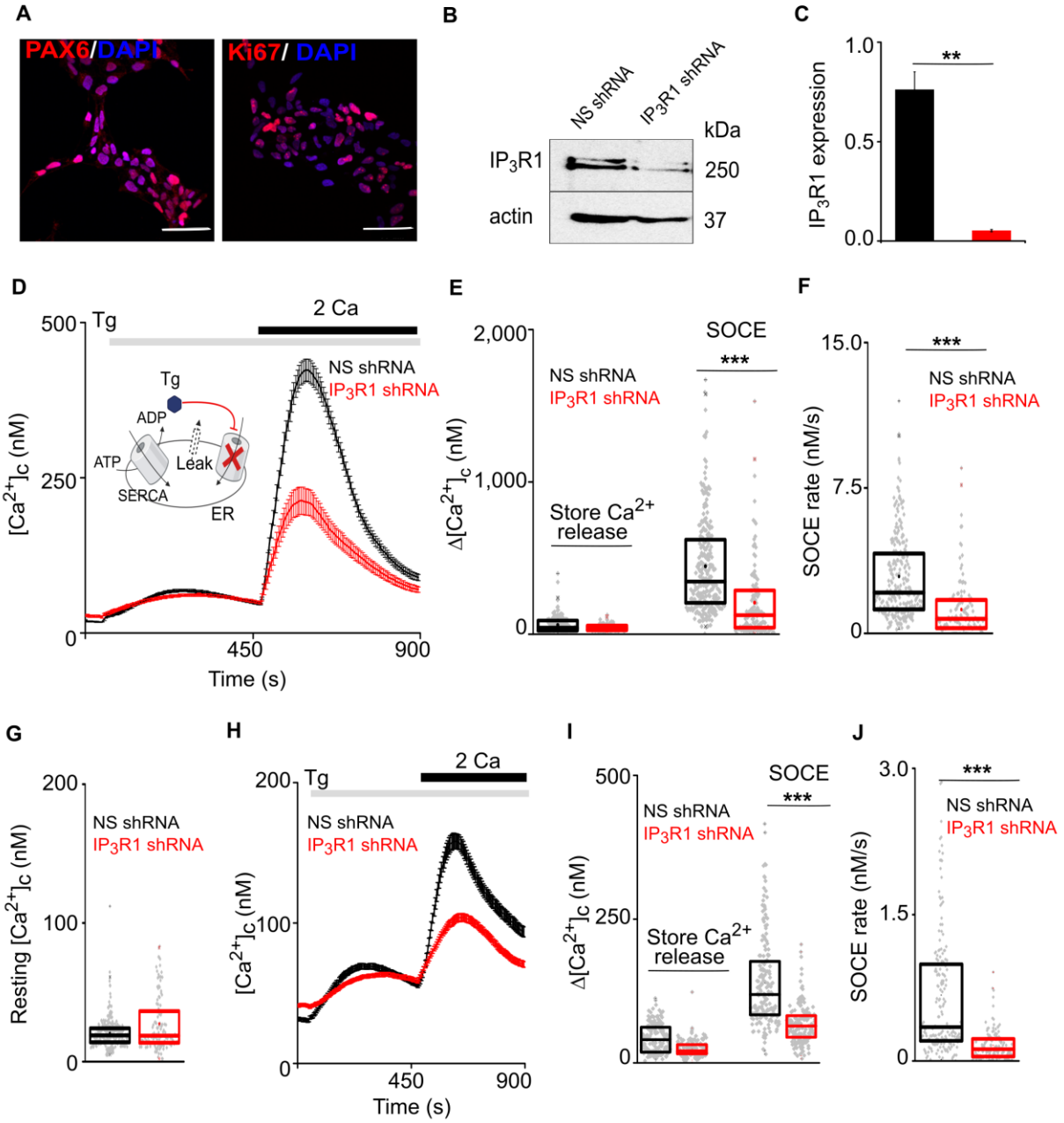
A
PAX6/DAPI
Ki67/ DAPI
B
NS shRNA
IP3R1 shRNA
kDa
IP3R1
250
actin
37
C
IP3R1 expression
1.0
0.5
0.0
**
D
Tg
2 Ca
500
250
0
[Ca2+]c (nM)
NS shRNA
IP3R1 shRNA
ADP
ATP
Leak
SERCA
ER
450
900
Time (s)
E
SOCE
2,000
1,000
0
Δ[Ca2+]c (nM)
NS shRNA
IP3R1 shRNA
***
Store Ca2+ release
F
15.0
7.5
0
SOCE rate (nM/s)
***
NS shRNA
IP3R1 shRNA
G
200
100
0
Resting [Ca2+]c (nM)
NS shRNA
IP3R1 shRNA
H
Tg
2 Ca
200
100
0
[Ca2+]c (nM)
NS shRNA
IP3R1 shRNA
450
900
Time (s)
I
SOCE
500
250
0
Δ[Ca2+]c (nM)
NS shRNA
IP3R1 shRNA
***
Store Ca2+ release
J
3.0
1.5
0
SOCE rate (nM/s)
***
NS shRNA
IP3R1 shRNA

Figure 2

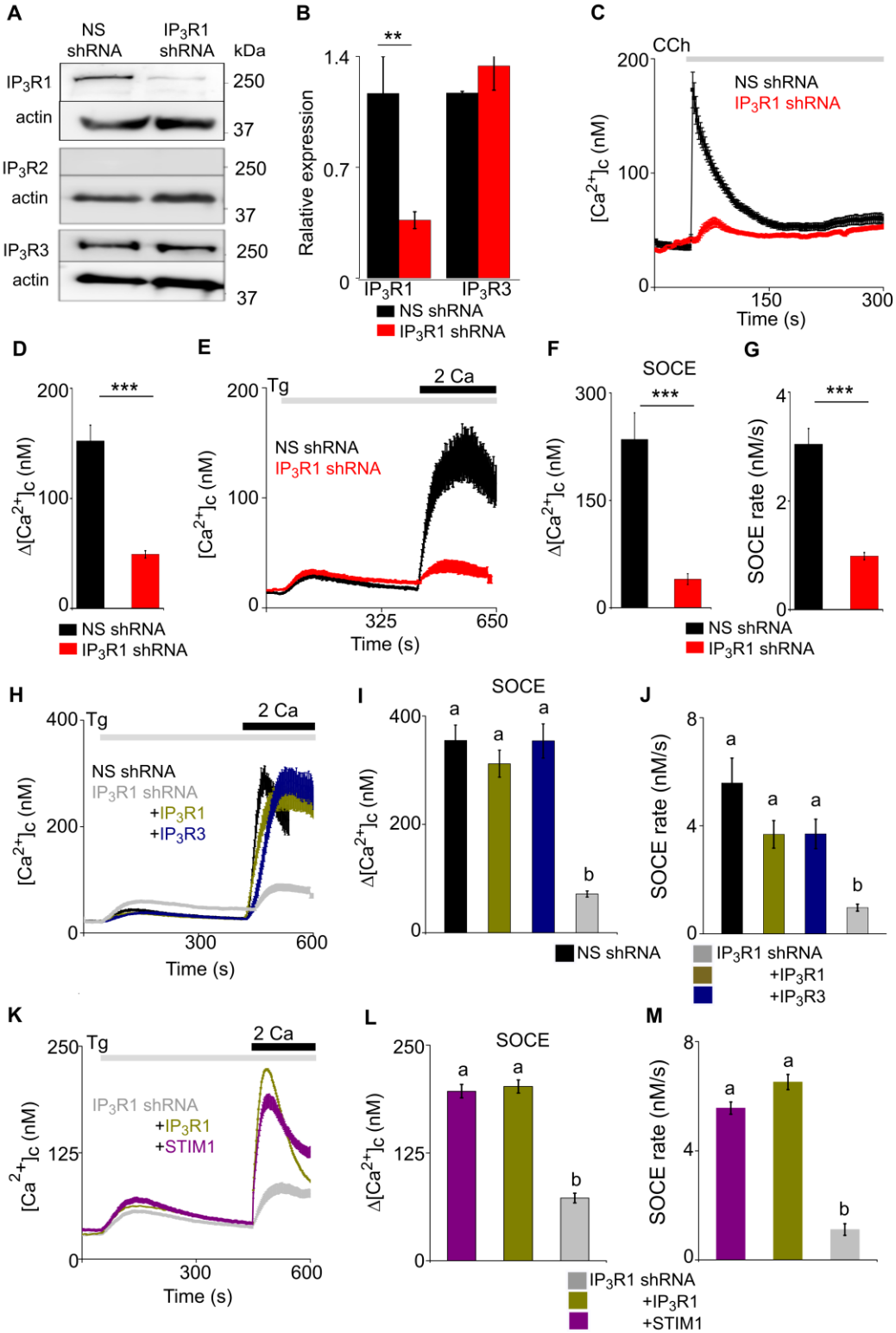
A
NS shRNA
IP3R1 shRNA
kDa
IP3R1
actin
IP3R2
IP3R3
250
37
B
**
Ralative expression
1.4
0.7
0
IP3R1
IP3R3
NS shRNA
IP3R1 shRNA
C
CCh
NS shRNA
IP3R1 shRNA
[Ca2+]c (nM)
200
100
0
150
300
Time (s)
D
***
Δ[Ca2+]c (nM)
200
100
0
NS shRNA
IP3R1 shRNA
E
Tg
2 Ca
NS shRNA
IP3R1 shRNA
[Ca2+]c (nM)
200
100
0
325
650
Time (s)
F
SOCE
***
Δ[Ca2+]c (nM)
300
150
0
G
***
SOCE rate (nM/s)
4
2
0
NS shRNA
IP3R1 shRNA
H
Tg
2 Ca
NS shRNA
IP3R1 shRNA
+IP3R1
+IP3R3
[Ca2+]c (nM)
400
200
0
300
600
Time (s)
I
SOCE
Δ[Ca2+]c (nM)
400
200
0
a
a
a
b
NS shRNA
J
SOCE rate (nM/s)
8
4
0
a
a
a
b
IP3R1 shRNA
+IP3R1
+IP3R3
K
Tg
2 Ca
IP3R1 shRNA
+IP3R1
+STIM1
[Ca2+]c (nM)
250
125
0
300
600
Time (s)
L
SOCE
Δ[Ca2+]c (nM)
250
125
0
a
a
b
IP3R1 shRNA
+IP3R1
+STIM1
M
SOCE rate (nM/s)
8
4
0
a
a
b

Figure 3

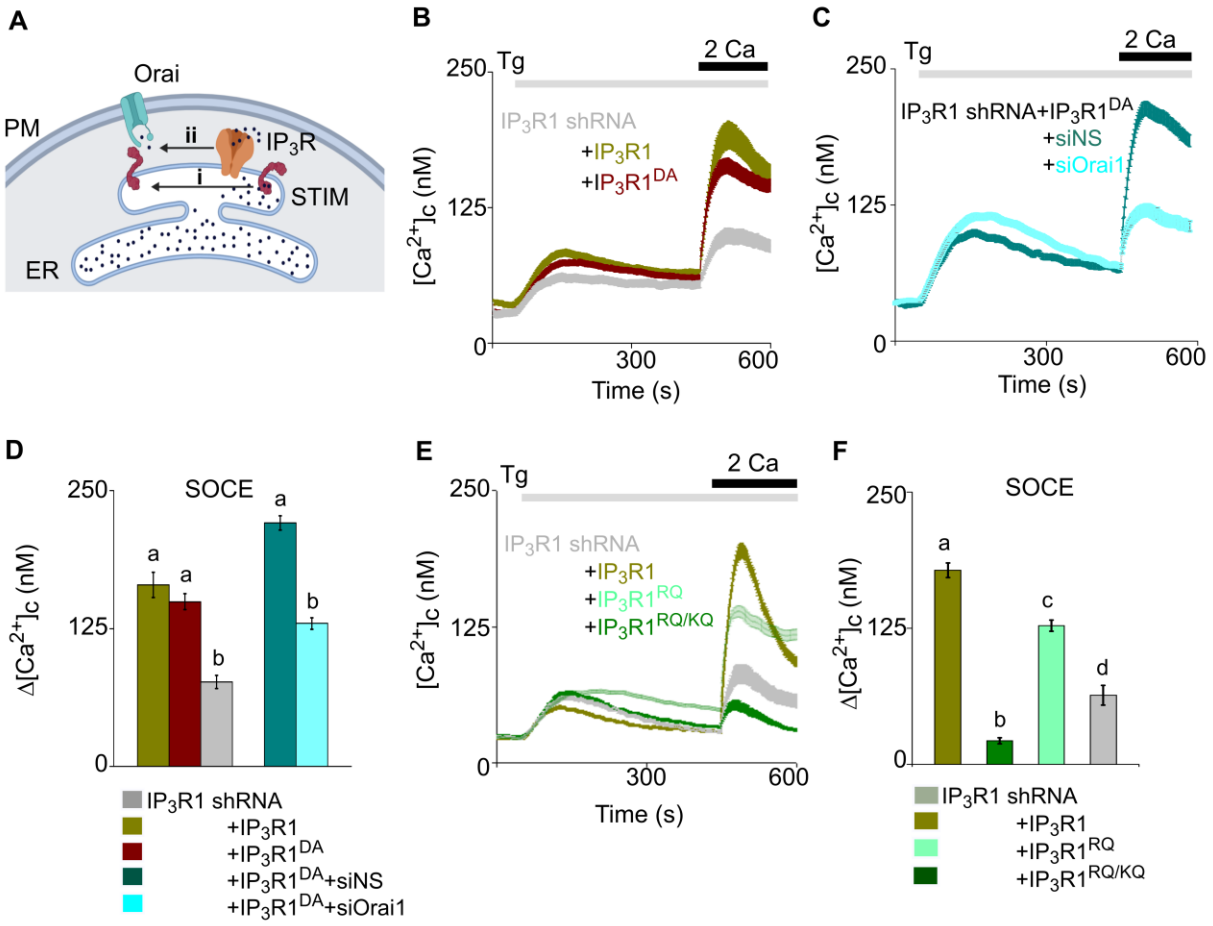
A
Orai
PM
ii
IP3R
i
STIM
ER
B
Tg
2 Ca
IP3R1 shRNA
+IP3R1
+IP3R1DA
[Ca2+]c (nM)
250
125
0
300
600
Time (s)
C
Tg
2 Ca
IP3R1 shRNA+IP3R1DA
+siNS
+siOrai1
[Ca2+]c (nM)
250
125
0
300
600
Time (s)
D
SOCE
Δ[Ca2+]c (nM)
250
125
0
a
a
b
a
b
IP3R1 shRNA
+IP3R1
+IP3R1DA
+IP3R1DA+siNS
+IP3R1DA+siOrai1
E
Tg
2 Ca
IP3R1 shRNA
+IP3R1
+IP3R1RQ
+IP3R1RQ/KQ
[Ca2+]c (nM)
250
125
0
300
600
Time (s)
F
SOCE
Δ[Ca2+]c (nM)
250
125
0
a
b
c
d
IP3R1 shRNA
+IP3R1
+IP3R1RQ
+IP3R1RQ/KQ

Figure 4

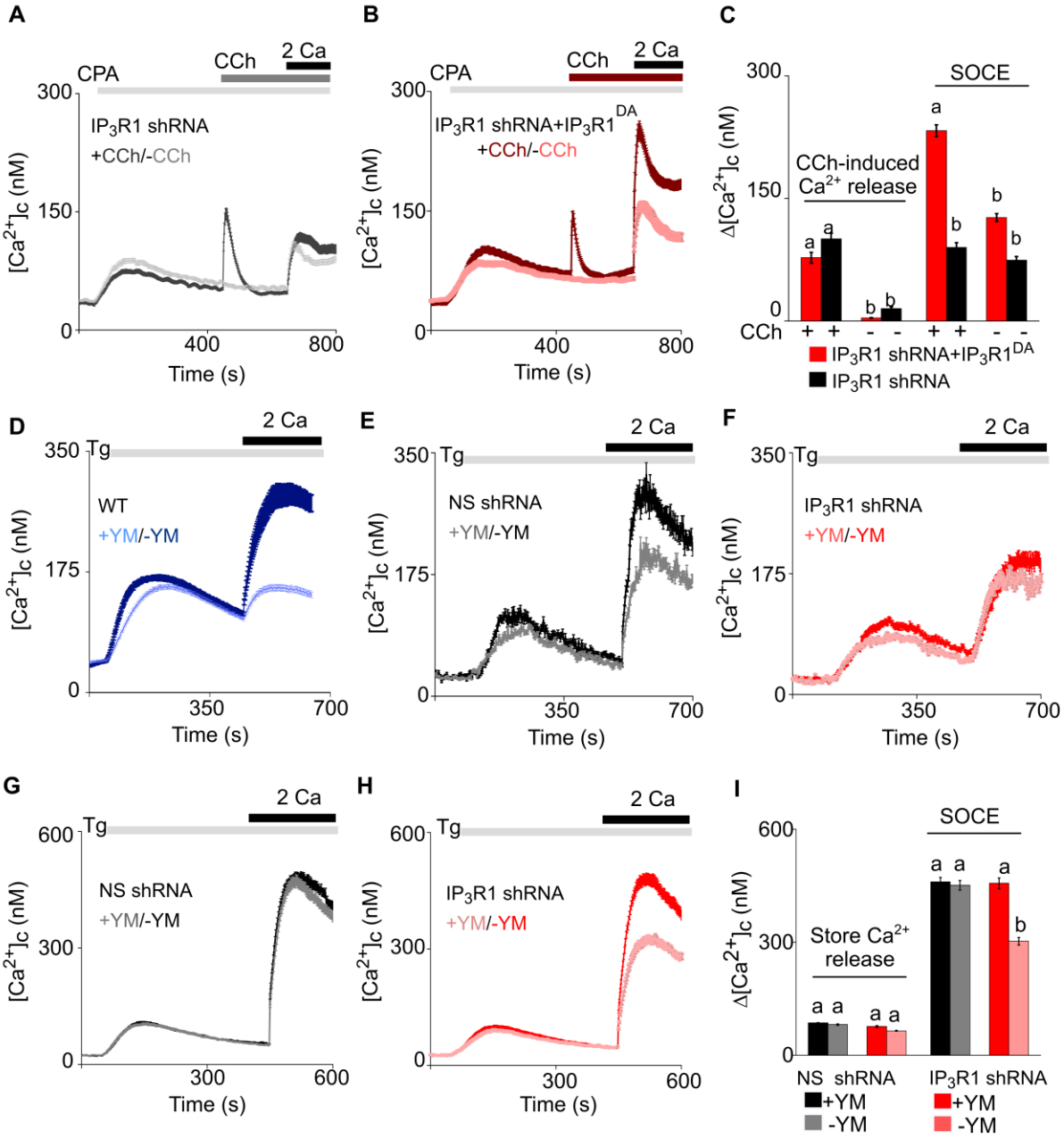
A
CPA
CCh
2 Ca
IP3R1 shRNA
+CCh/-CCh
[Ca2+]c (nM)
Time (s)
B
CPA
CCh
2 Ca
IP3R1 shRNA+IP3R1DA
+CCh/-CCh
[Ca2+]c (nM)
Time (s)
C
SOCE
CCh-induced
Ca2+ release
Δ[Ca2+]c (nM)
CCh
IP3R1 shRNA+IP3R1DA
IP3R1 shRNA
D
Tg
2 Ca
WT
+YM/-YM
[Ca2+]c (nM)
Time (s)
E
Tg
2 Ca
NS shRNA
+YM/-YM
[Ca2+]c (nM)
Time (s)
F
Tg
2 Ca
IP3R1 shRNA
+YM/-YM
[Ca2+]c (nM)
Time (s)
G
Tg
2 Ca
NS shRNA
+YM/-YM
[Ca2+]c (nM)
Time (s)
H
Tg
2 Ca
IP3R1 shRNA
+YM/-YM
[Ca2+]c (nM)
Time (s)
I
SOCE
Store Ca2+
release
Δ[Ca2+]c (nM)
NS shRNA
IP3R1 shRNA
+YM
-YM
+YM
-YM

Figure 5

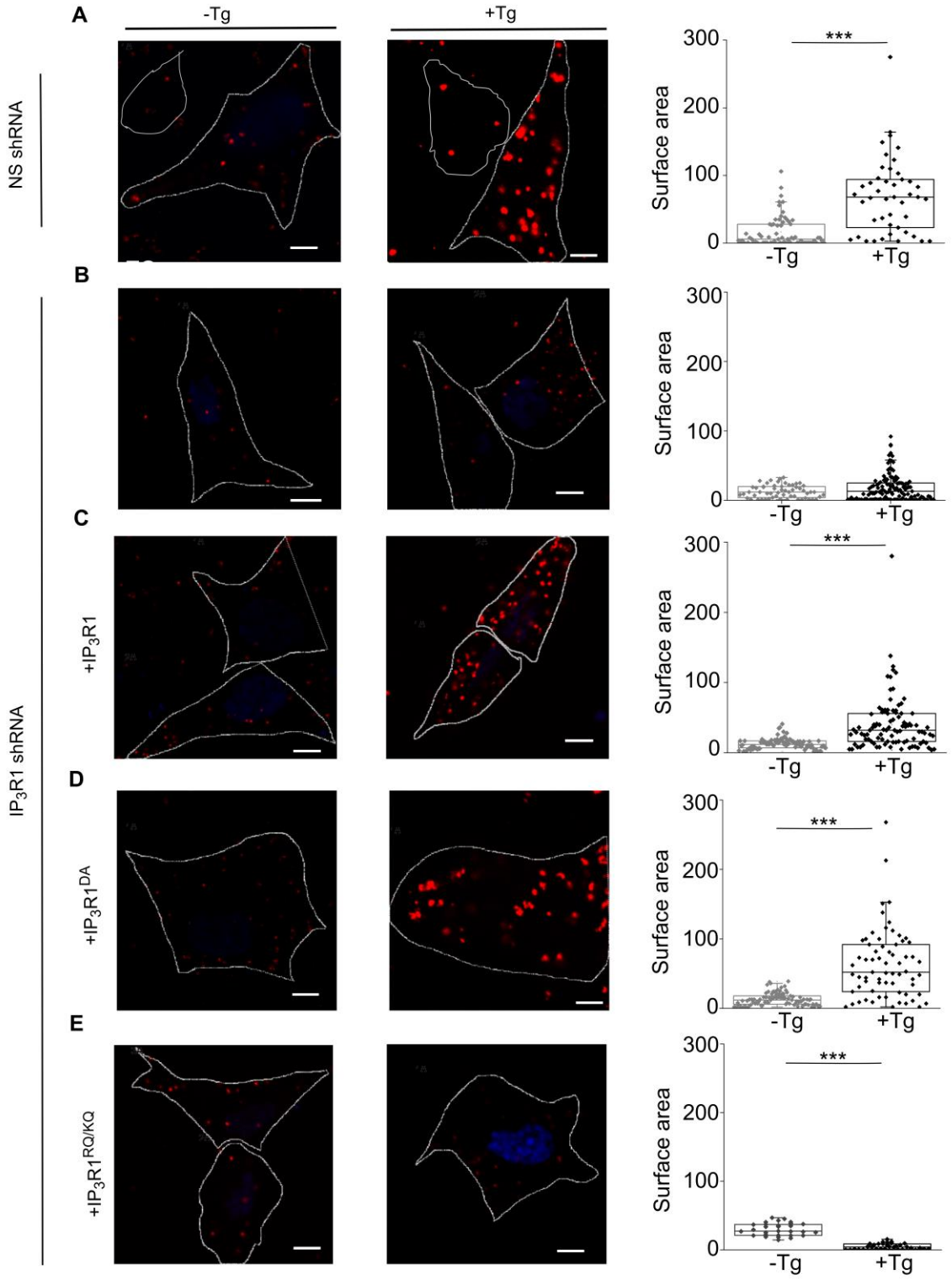
A
-Tg
+Tg
NS shRNA
Surface area
300
200
100
0
***
-Tg
+Tg
B
IP3R1 shRNA
C
+IP3R1
D
+IP3R1DA
E
+IP3R1RQ/KQ

Figure 6

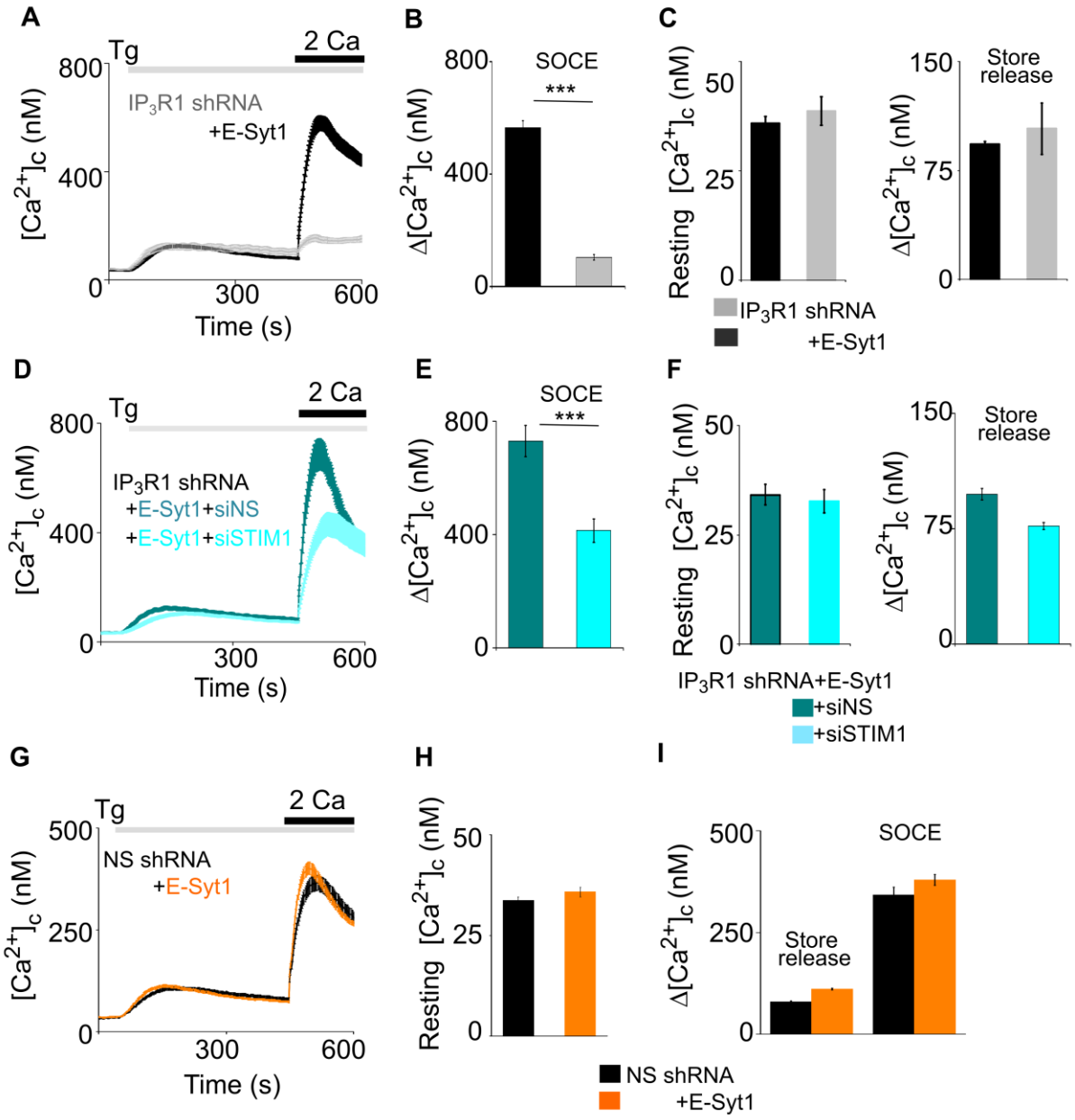
A
Tg
2 Ca
IP3R1 shRNA
+E-Syt1
[Ca2+]c (nM)
800
400
0
300
600
Time (s)
B
SOCE
***
Δ[Ca2+]c (nM)
800
400
0
C
Resting [Ca2+]c (nM)
50
25
0
Store release
150
75
0
IP3R1 shRNA
+E-Syt1
D
Tg
2 Ca
IP3R1 shRNA
+E-Syt1+siNS
+E-Syt1+siSTIM1
[Ca2+]c (nM)
800
400
0
300
600
Time (s)
E
SOCE
***
Δ[Ca2+]c (nM)
800
400
0
F
Resting [Ca2+]c (nM)
50
25
0
Store release
150
75
0
IP3R1 shRNA+E-Syt1
+siNS
+siSTIM1
G
Tg
2 Ca
NS shRNA
+E-Syt1
[Ca2+]c (nM)
500
250
0
300
600
Time (s)
H
Resting [Ca2+]c (nM)
50
25
0
I
SOCE
Store release
Δ[Ca2+]c (nM)
500
250
0
NS shRNA
+E-Syt1

Figure 7

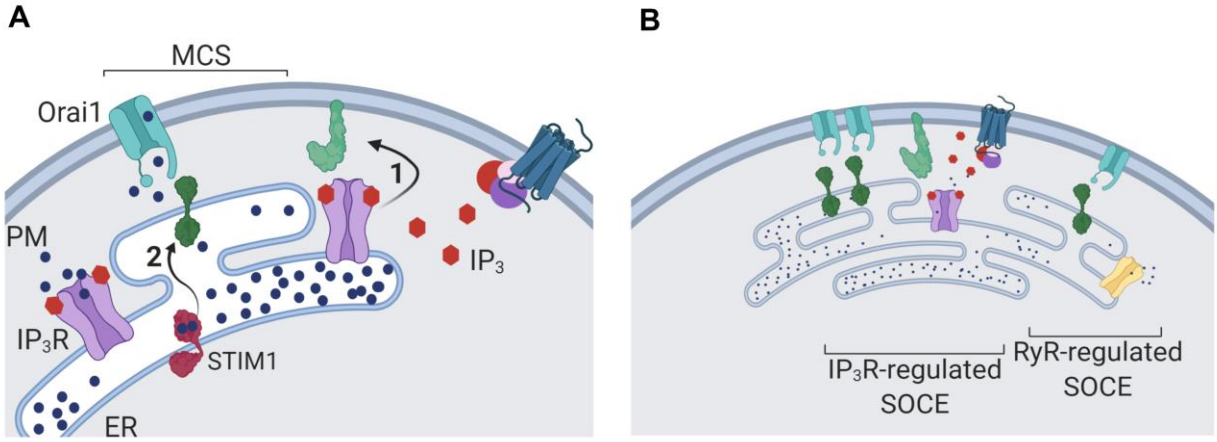
A
MCS
Orai1
PM
1
2
IP3
IP3R
STIM1
ER
B
IP3R-regulated
SOCE
RyR-regulated
SOCE

Figure 1 figure supplement 1

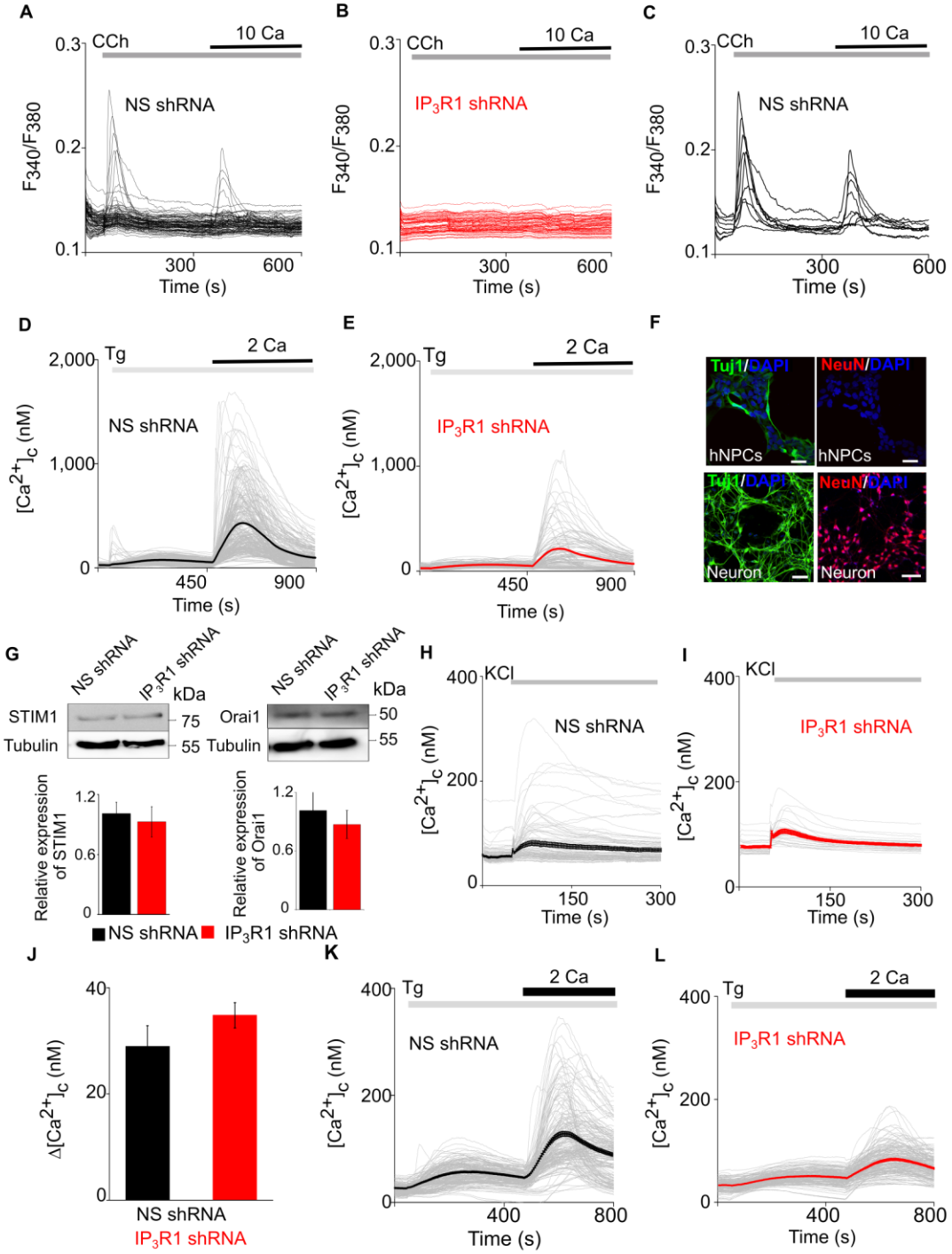

Figure 2-figure supplement 1

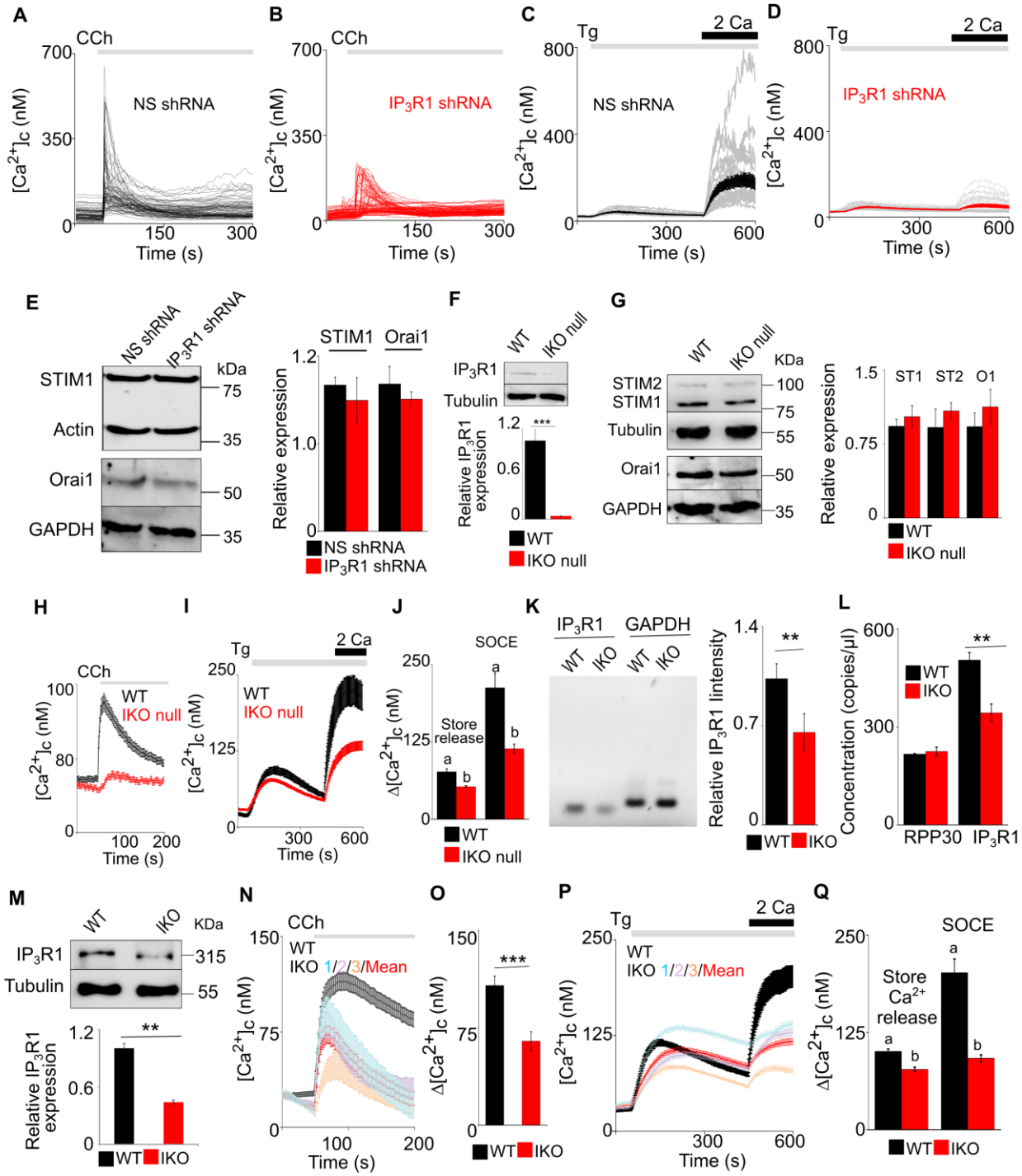

Figure 2-figure supplement 2

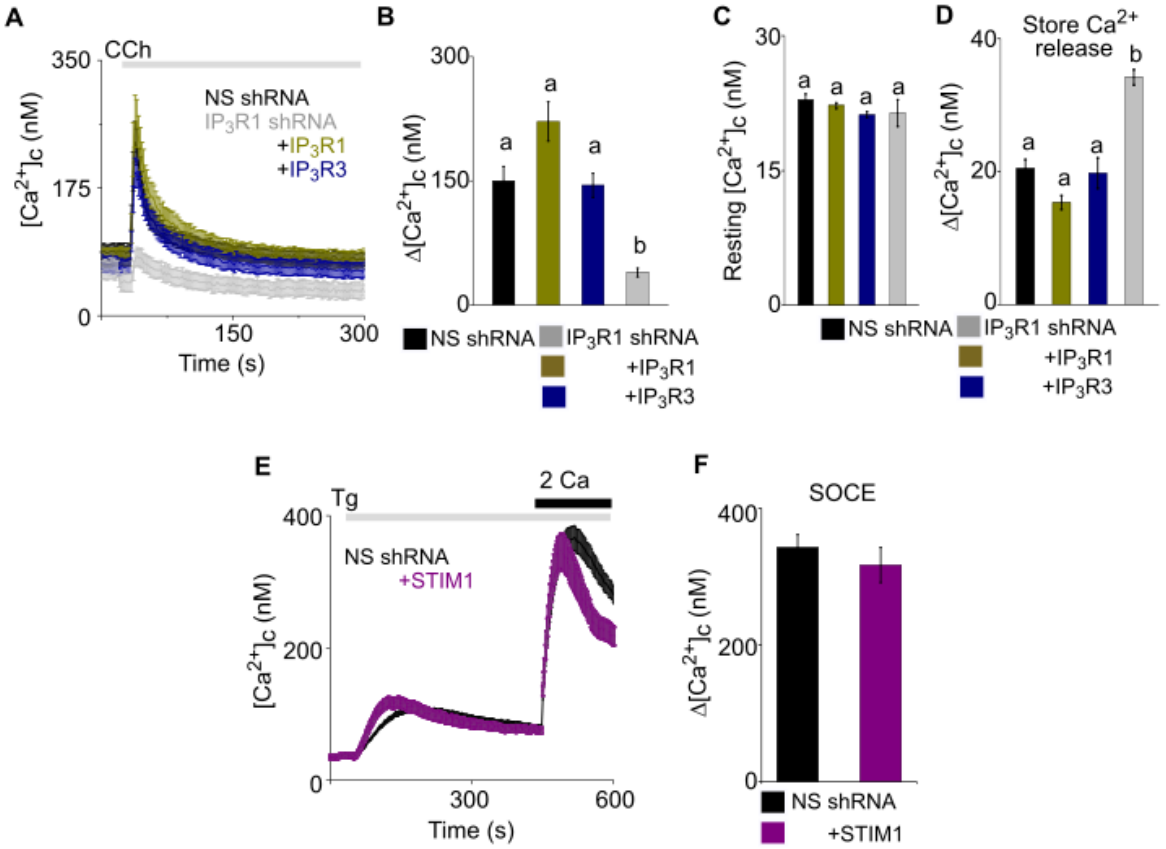

Figure 2-figure supplement 3

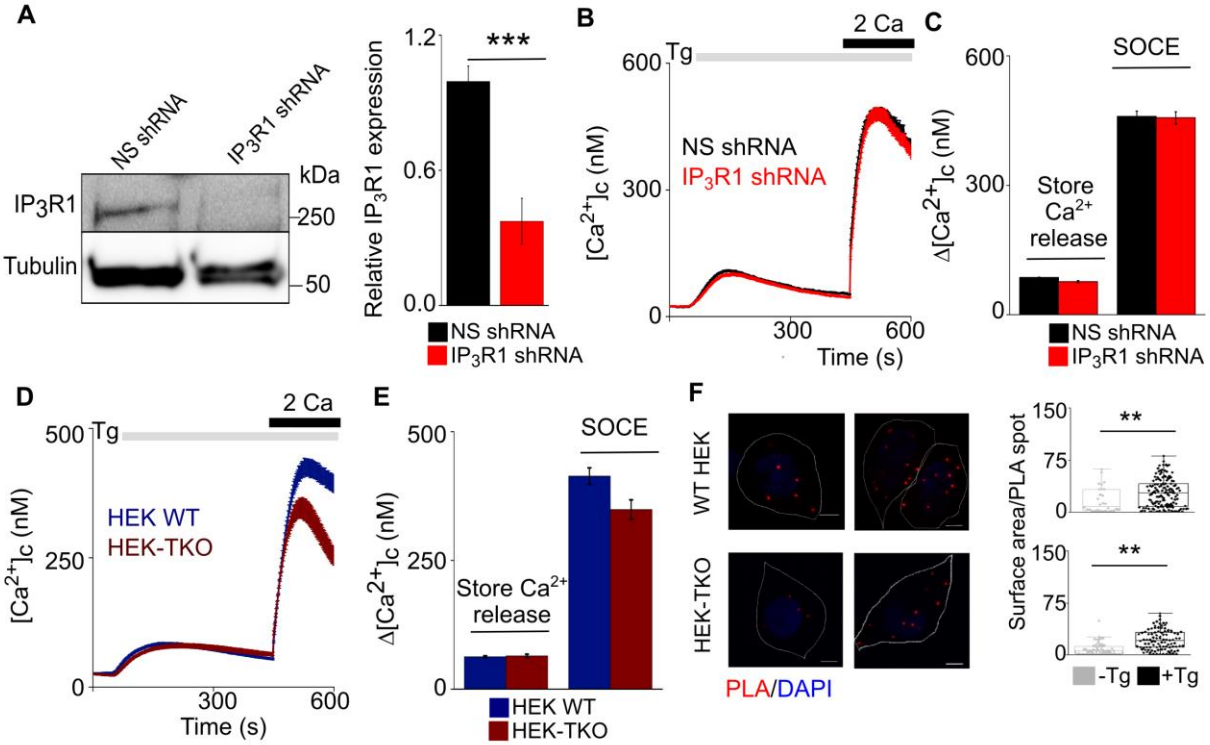

Figure 3-figure supplement 1

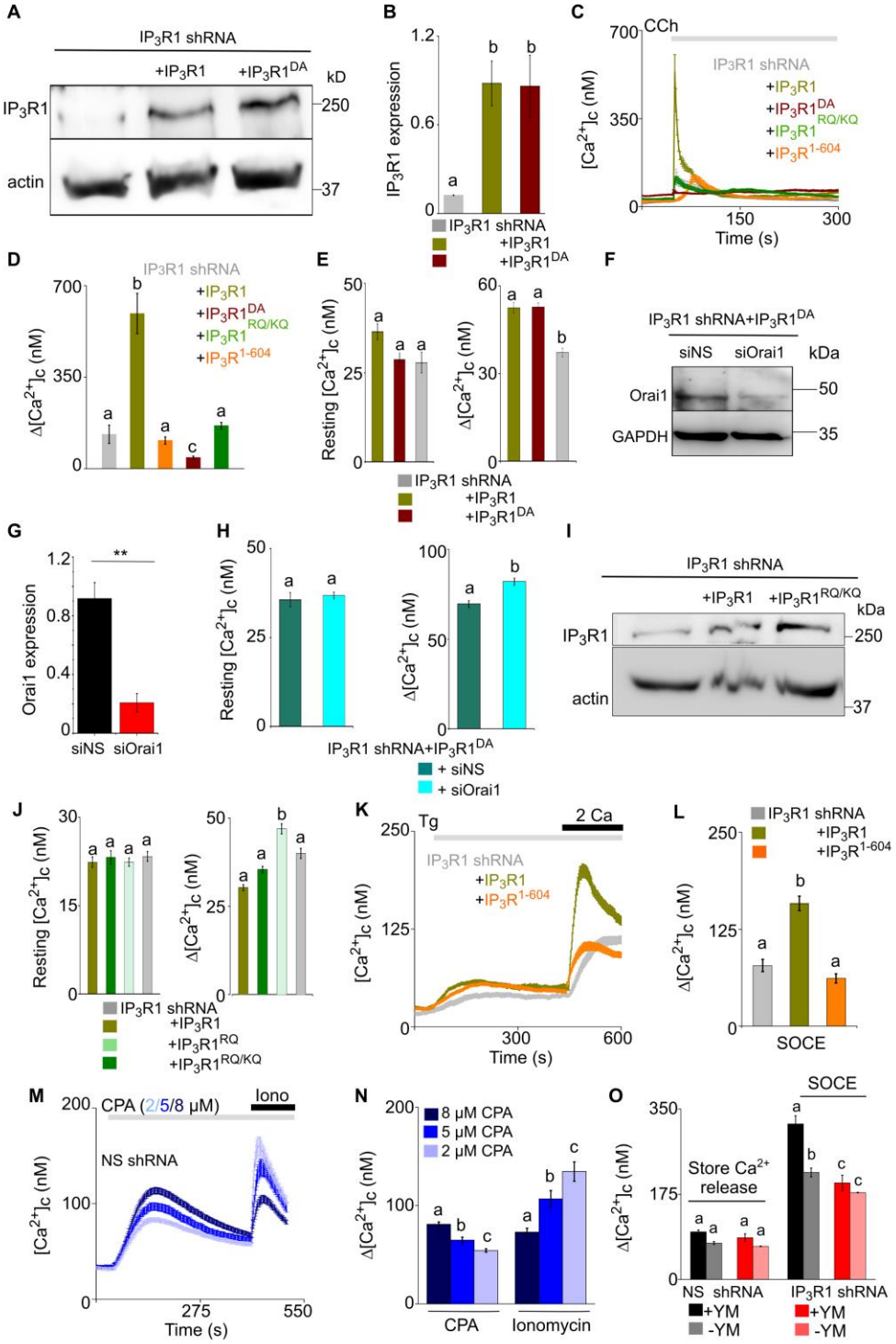

Figure 4-figure supplement 1

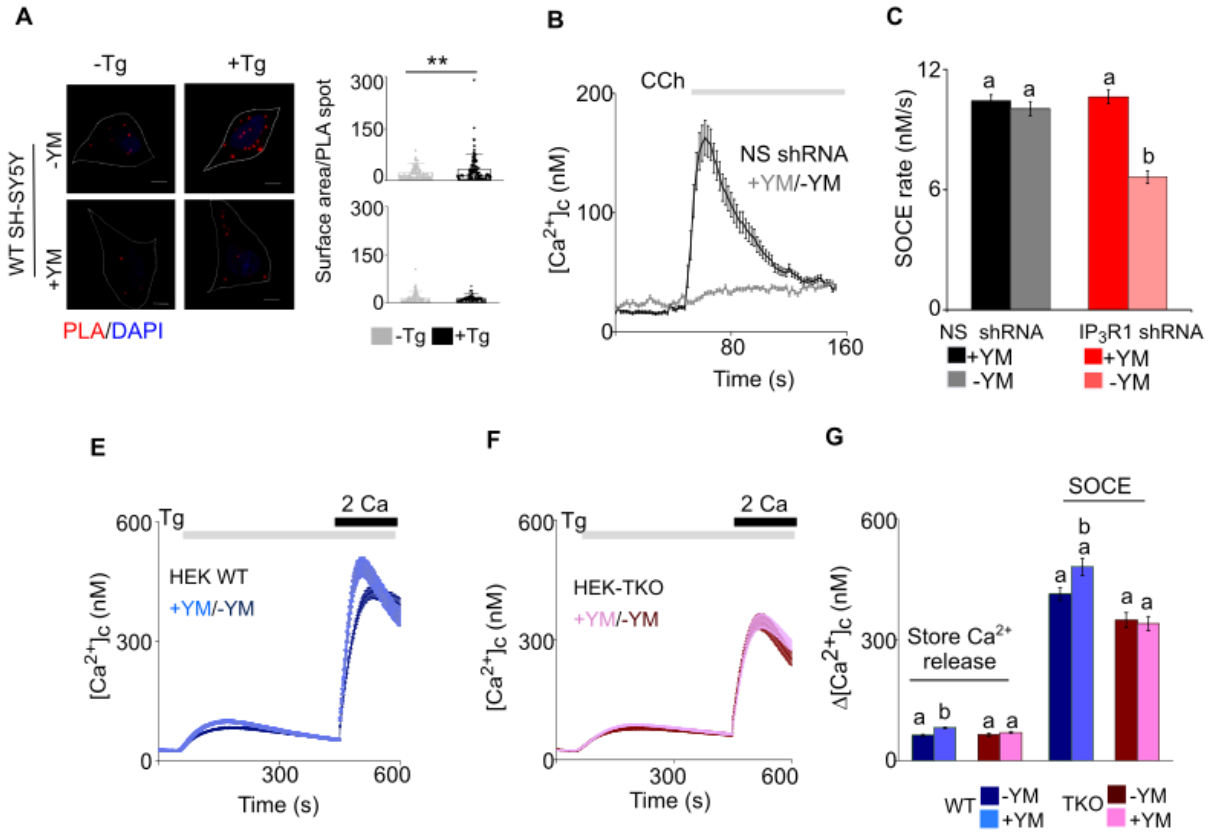
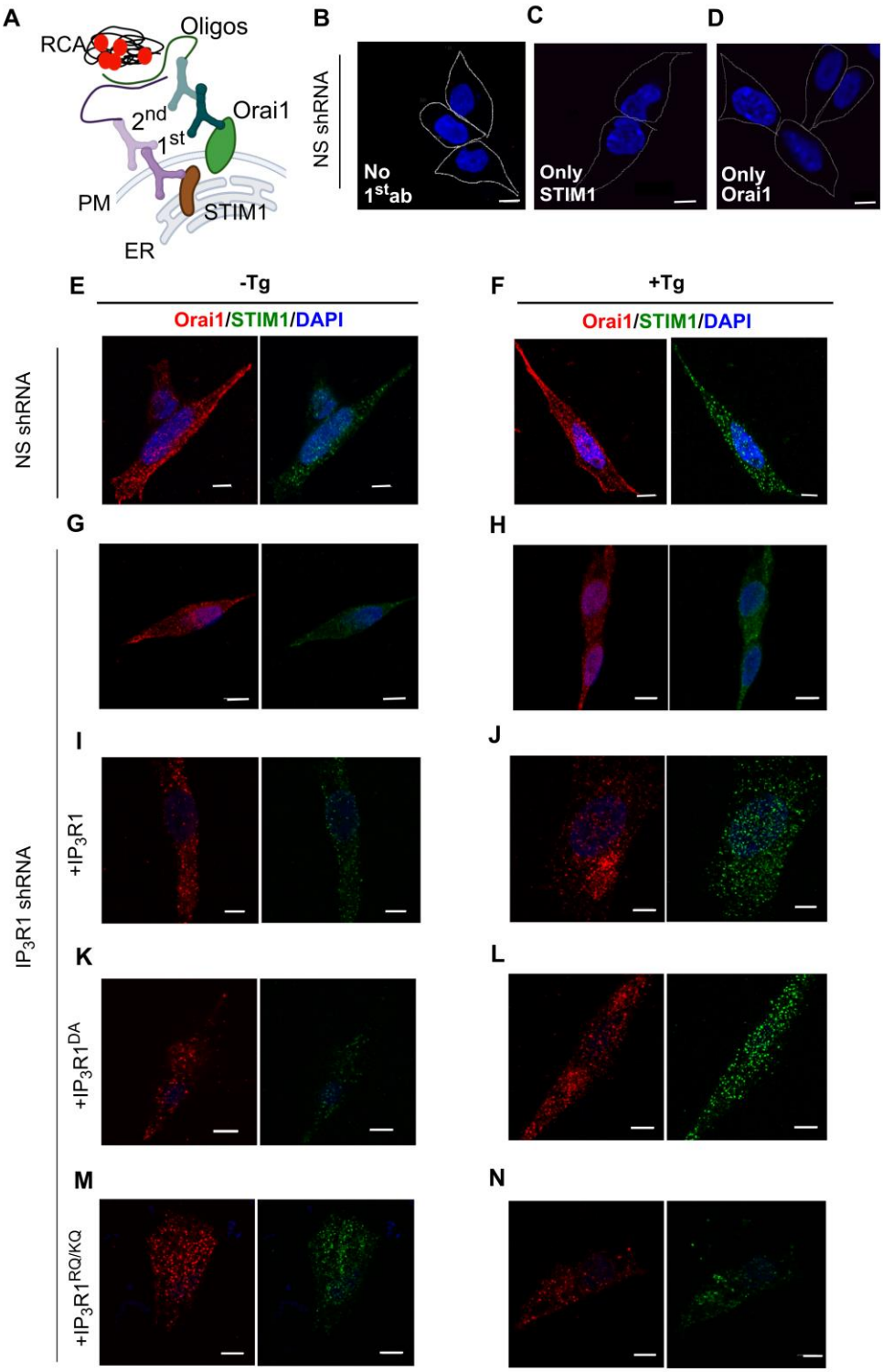
Figure 5-figure supplement 1